

SOCKET: SOft Collision Kernel EsTimator for Sparse Attention

Sahil Joshi* Agniva Chowdhury* Wyatt Bellinger* Amar Kanakamedala*
Ekam Singh* Hoang Anh Duy Le* Aditya Desai[†] Anshumali Shrivastava*

Abstract

Exploiting sparsity during long-context inference is central to scaling large language models, as attention dominates the cost of autoregressive decoding. Sparse attention reduces this cost by restricting computation to a subset of tokens, but its effectiveness depends critically on efficient scoring and selection of relevant tokens at inference time. We revisit Locality-Sensitive Hashing (LSH) as a sparsification primitive and introduce SOCKET, a SOft Collision Kernel EsTimator that replaces hard bucket matches with probabilistic, similarity-aware aggregation. Our key insight is that hard LSH produces discrete collision signals and is therefore poorly suited for ranking. In contrast, soft LSH aggregates graded collision evidence across hash tables, preserving the stability of relative ordering among the true top- k tokens. This transformation elevates LSH from a candidate-generation heuristic to a principled and mathematically grounded scoring kernel for sparse attention. Leveraging this property, SOCKET enables efficient token selection without ad-hoc voting mechanism, and matches or surpasses established sparse attention baselines across multiple long-context benchmarks using diverse set of models. With a custom CUDA kernel for scoring keys and a Flash Decode Triton backend for sparse attention, SOCKET achieves up to 1.5 \times higher throughput than FlashAttention, making it an effective tool for long-context inference. Code is open-sourced at <https://github.com/amarka8/SOCKET>.

1 Introduction

Large language models (LLMs), such as GPT [4] and Llama [43], have achieved remarkable performance in next-token prediction, enabling a wide range of applications in language understanding and generation [37, 8, 20, 33]. To support more powerful in-context learning and increasingly complex applications [4, 45, 15, 35, 38], the maximum input length supported during inference has grown rapidly—from 2K–4K tokens [44, 14] to 32K [2, 8], 128K [43, 33], and even millions of tokens [30]. Beyond language, LLMs have also been extended to multimodal domains such as vision, video, code, databases, and scientific discovery [36, 27, 39, 28, 54, 25].

LLM inference consists of an initial prefilling phase followed by iterative decoding steps that generate one token at a time. During prefilling, the model processes the full input sequence and computes key–value (KV) representations for all tokens. During decoding, only the most recently generated token is processed, and its KV representations are appended to the cache, avoiding redundant computation. However, each decoding step requires the new token to attend to all previously cached tokens, making attention computation increasingly memory-bound as the context grows. When the KV cache exceeds GPU memory capacity and is partially offloaded to CPU memory, additional CPU–GPU transfers further exacerbate this bottleneck. These effects reveal a fundamental scalability limitation of dense attention for long-context inference. Sparse attention addresses this limitation by restricting attention to a selected subset of tokens, reducing memory movement while approximating dense attention behavior.

*Department of Computer Science, Rice University, TX, USA. {sj157, ac508, wb20, ask20, es100, el72, as143}@rice.edu

[†]Department of Electrical Engineering and Computer Sciences, UC Berkeley, CA, USA. apdesai@berkeley.edu

Table 1: Performance across sparsity levels on RULER-32K (Llama-3.1-8B-Instruct). Mem denotes additional memory (bits/token) beyond the KV cache. Spr denotes sparsity.

Method	Spr	Mem	nm2	nm3	vt	fwe	qa1	qa2	avg
PQcache	5×	256	100	99	98.2	92.7	81	51	86.9
Quest	5×	512	100	99	97.6	89.7	85	54	87.5
DS	5×	512	91	98	97.8	93.0	81	51	85.3
HashAttn	5×	128	97	97	94.2	93.7	83	49	85.6
MagicPig	5×	1024	10	0	82.8	91.7	38	42	44.1
SOCKET	5×	600	97	100	95.2	91.7	84	53	86.8
PQcache	10×	256	98	99	96.4	92.3	81	51	86.2
Quest	10×	512	100	99	95.0	88.3	86	53	86.8
DS	10×	512	91	97	95.2	92.3	74	51	83.4
HashAttn	10×	128	87	86	88.6	92.3	79	50	80.4
MagicPig	10×	1024	2	0	32.2	83.0	35	29	30.2
SOCKET	10×	600	95	100	94.2	88.7	82	53	85.5
PQcache	20×	256	93	92	94.2	87.7	82	50	83.1
Quest	20×	512	90	96	91.4	87.7	84	54	83.8
DS	20×	512	49	82	90.2	92.3	68	51	72.0
HashAttn	20×	128	73	45	81.0	89.7	75	51	69.1
MagicPig	20×	1024	2	0	0.0	83.0	35	29	24.8
SOCKET	20×	600	93	92	91.4	86.0	82	52	82.7
PQcache	50×	256	64	62	86.0	83.3	73	49	69.5
Quest	50×	512	74	30	76.0	80.0	71	54	64.1
DS	50×	512	20	1	66.4	88.3	48	44	44.6
HashAttn	50×	128	32	0	72.2	83.7	63	46	49.4
MagicPig	50×	1024	1	0	0.0	61.7	11	24	16.2
SOCKET	50×	600	83	74	83.6	64.0	77	50	71.9

The attention output for a query \mathbf{q} under scaled dot-product attention (SDPA) is given by

$$\mathbf{y}(\mathbf{q}) = \sum_{i=1}^n \alpha_i \mathbf{v}_i, \quad (1)$$

where $\alpha_i = \exp(\mathbf{k}_i^\top \mathbf{q}) / \sum_{j=1}^n \exp(\mathbf{k}_j^\top \mathbf{q})$ and, $\mathbf{k}_i, \mathbf{v}_i \in \mathbb{R}^d$ denote the key and value vectors associated with token i , and α_i represents its attention weight. The central challenge in approximating dense attention lies in identifying the tokens that contribute most to this sum. Prior work has shown that, in hindsight, the dominant contributors are those with large values of $\alpha_i \|\mathbf{v}_i\|_2^2$ [13]. This observation motivates selecting tokens with the largest query–key inner products $\mathbf{k}_i^\top \mathbf{q}$, commonly referred to as *top- k* selection. Related extensions, such as top- p , further adapt this strategy by dynamically allocating token budgets across attention heads. Consequently, much of the sparse attention literature has focused on efficiently approximating top- k selection [42, 51, 52, 13, 21, 19] or top- p selection [55]. Locality-Sensitive Hashing (LSH) [23], in particular, is a widely used randomized technique for identifying similar keys in high-dimensional spaces. In its traditional form, LSH applies random projections followed by a sign function, producing binary collision indicators between a query and a key. However, this *hard* formulation is poorly suited for ranking stability of important keys: binary collisions cannot express partial similarity, leading to coarse and noisy rankings (see fig. 2). Soft LSH resolves this limitation by aggregating collision evidence across multiple hash tables to produce lightweight, similarity-aware scores for every key. Recently, randomized data structures have emerged as a promising approach for approximating attention. RACE-based sketches [9, 10] have been used to approximate softmax attention in linear time [24], while LSH-based methods have been explored to approximate attention and retrieval [26, 17, 31]. These works highlight the potential of randomized, data-independent

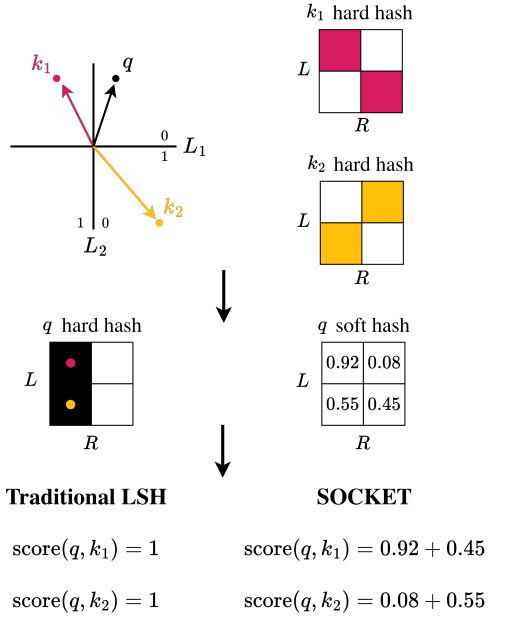


Figure 1: Traditional LSH assigns binary scores via hash collisions, whereas soft LSH produces continuous scores through probabilistic bucket assignments, resulting in a stable ranking.

primitives to reduce attention cost without relying on expensive data-dependent preprocessing. Unlike most existing sparse attention methods, SOCKET is *data-agnostic*. This design choice yields three key advantages. First, it enables substantially faster index construction compared to data-dependent clustering approaches such as k -means, as shown in fig. 3a. Second, it enables deployment without retraining or calibration, making it robust to distribution shifts during inference. Finally, it allows for interpretable theoretical guarantees with respect to a kernel that closely approximates the softmax kernel, as formalized in Theorem 3.

Key Idea: Our preliminary experiments with a *hard* LSH-based scorer show that it fails to rank candidate keys according to their true importance, as illustrated in fig. 2. This observation motivates a re-examination of the role of LSH in sparse attention and raises a fundamental question: *Can we augment traditional LSH to more effectively rank candidates by their relevance?*

In SOCKET, each key is assigned a continuous score derived from soft collision probabilities of a query across multiple hash tables, weighted by the corresponding value vector norms. This formulation transforms LSH from a binary decision process into a principled, similarity-aware scoring kernel that enables stable ranking of keys. These scores enable efficient key selection without accessing full key or value vectors. From a systems perspective, this distinction is critical: exact top- k selection requires reading entire key vectors (e.g., 128 bfloat values per token), whereas SOCKET selects importance keys by reading only a single bfloat (soft count) and a single integer per key (value vector norm), dramatically reducing memory traffic during decoding while preserving ranking fidelity. To evaluate ranking quality, we analyze the ground-truth scores of the keys *i.e.*, $\mathbf{q}^\top \mathbf{k}$ selected in the top- k by each method. Fig. 2d plots histograms of ground-truth attention scores for the keys selected by SOCKET and hard LSH, with the dashed line marking the ground-truth k -th score. Scores exceeding this threshold correspond to true top- k keys. Methods that concentrate more mass beyond the cutoff therefore yield higher-quality rankings. SOCKET exhibits this behavior, indicating that *soft* LSH provides a stable importance ranking and supports accurate and efficient sparse attention. In addition to our novel findings about SOCKET and extensive empirical validation, we make the following contributions:

I. Soft LSH as a *stable ranker*: We propose a *data-agnostic soft* LSH mechanism that serves as a substantially more effective ranking function than traditional hard LSH, making it well suited for sparse attention.

II. Efficiency with SOCKET: We present a custom CUDA kernel for scoring of keys and show a 1.5 \times throughput speedup over FlashAttention during decoding.

III. Theoretical Insights: We provide theoretical guarantees showing that attention computed using soft LSH scores closely approximates a kernel that is very similar to softmax.

2 Related Work

Due to the importance of long-context inference, a substantial body of prior work accelerates attention by approximating top- k selection and restricting computation to a small subset of tokens per query. Since identifying the top- k tokens with the highest attention scores naively requires $\mathcal{O}(nd)$ computation, where n is the number of tokens in the key-value cache and d is the embedding size, several methods reduce either the effective dimensionality or the number of tokens considered. One line of work addresses this problem by approximating top- k selection using dimensionality reduction techniques. DOUBLE SPARSITY [51] reduces computation along the feature dimension by selecting a subset of channels to estimate query–key dot products, where channels are chosen via offline calibration of channel norms. QUEST [42] reduces computation along the token dimension by constructing page-level representations and selecting or discarding all tokens within a page jointly. While both approaches are effective in practice, they rely on data-dependent heuristics and do not provide the-

oretical guarantees on the resulting attention approximation. In Section 6, we show that SOCKET matches or outperforms these methods using Llama-3.1-8B-Instruct and Qwen3-8B while offering a principled, data-agnostic alternative.

A second line of work frames top- k attention as a retrieval problem. RETRIEVALATTENTION [29] employs graph-based nearest neighbor search to identify tokens with large query–key inner products. However, due to the sparse and irregular nature of graph computations, top- k selection is offloaded to the CPU, introducing additional latency during decoding. PQCACHE [52] instead integrates product quantization (PQ) into KV-cache management to enable approximate retrieval of the most relevant keys, also relying on a CPU–GPU system design. In contrast to these data-dependent approaches, we show that *data-agnostic* random projections can significantly accelerate index construction while achieving comparable or improved accuracy. In Section 6, we demonstrate that SOCKET outperforms PQCACHE on Llama-3.1-8B-Instruct and Qwen3-8B, while offering a simpler alternative. Furthermore, several approaches estimate attention outputs using hashing-based data structures. LEARNING-TO-HASH ATTENTION [41] trains hash functions to map keys into balanced hash tables, enabling sparse retrieval during attention computation. HASHATTENTION [13] encodes queries and keys into Hamming space using learned mappings to capture semantic similarity. MAGICPIG [7] observes that hard top- k attention can be biased when attention scores are relatively uniform, and proposes an importance-sampling-based estimator that leverages LSH tables to approximate the sampling distribution. While these methods highlight the potential of hashing for reducing attention cost, they primarily rely on hard or learned hash functions and do not directly address the problem of accurate key ranking. In Section 6, we empirically demonstrate that SOCKET’s soft LSH-based scoring yields more reliable performance and improved attention approximation.

Several other works address the challenge of efficient long-context inference, including LOKI [40], SQUEEZEDATTENTION [21], INFLLM [46], H2O [53], STREAMLLM [47], ADAMAS [49], and vATTENTION [12]. These approaches explore complementary system- and algorithm-level techniques to reduce attention overhead during inference. Our goal in this work is not to provide a comprehensive empirical comparison against all such methods. Instead, we focus on developing a principled, data-agnostic sparsification technique that leverages locality-sensitive hashing as a similarity-aware scoring mechanism, rather than a binary filtering heuristic. Accordingly, we do not discuss these methods further.

3 Background

3.1 Locality-Sensitive Hashing (LSH)

An LSH family \mathcal{H} for a similarity Sim makes near pairs collide more often than far pairs. Formally, \mathcal{H} is (S_0, cS_0, p_1, p_2) -sensitive if for all $x, y \in \mathbb{R}^D$,

$$\begin{cases} \text{Sim}(x, y) \geq S_0 \Rightarrow \Pr_{h \sim \mathcal{H}}[h(x) = h(y)] \geq p_1, \\ \text{Sim}(x, y) \leq cS_0 \Rightarrow \Pr_{h \sim \mathcal{H}}[h(x) = h(y)] \leq p_2, \end{cases}$$

where $p_1 > p_2$ and $c < 1$. Such families enable sublinear-time approximate nearest-neighbor data structures. A convenient sufficient condition, satisfied by SimHash and WTA [5, 48, 6], is that the collision probability is a monotone function of similarity, $\Pr_{h \sim \mathcal{H}}[h(x) = h(y)] = f(\text{Sim}(x, y))$ with f increasing.

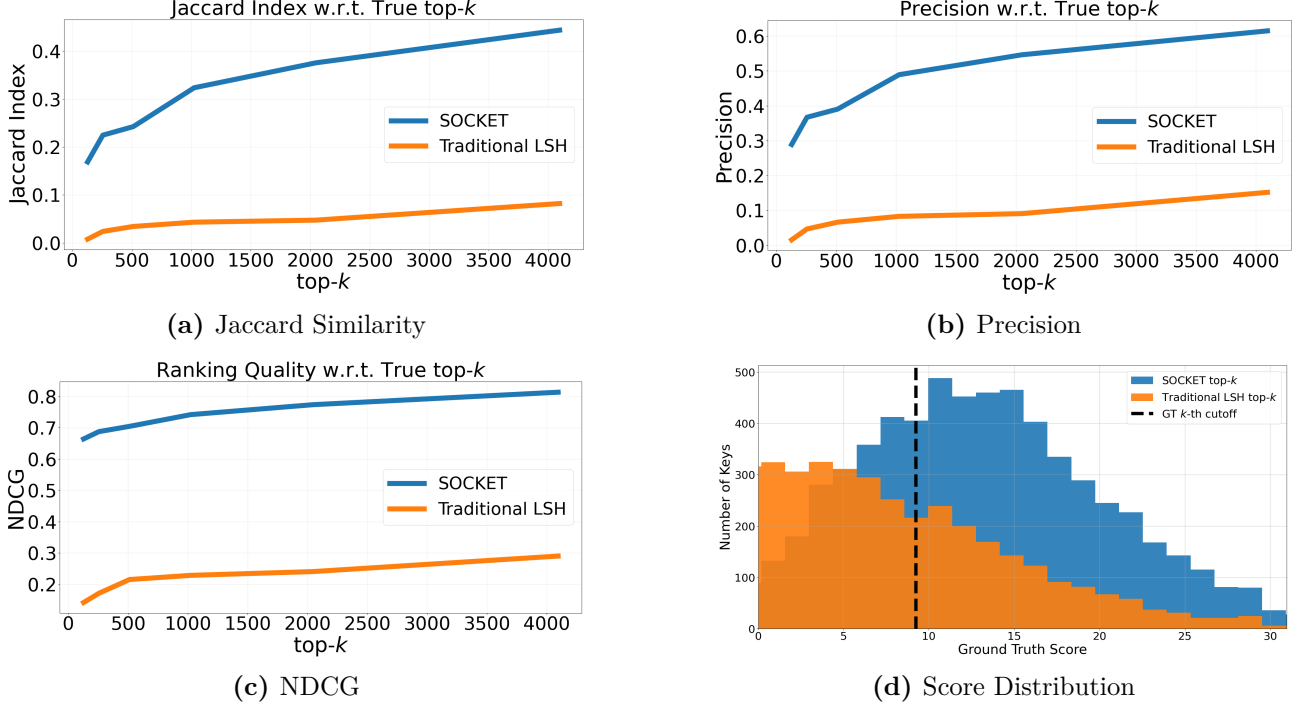


Figure 2: Ranking quality comparison between SOCKET and traditional LSH as a function of top- k . Keys are randomly generated using a standard Gaussian distribution, and ground-truth relevance is defined by dot-product similarity between a query and a key. (a)–(b) measure overlap with the ground-truth top- k set, while (c) additionally evaluates agreement with the ground-truth ranking. (d) shows ground-truth scores for the top- k keys selected by SOCKET and hard LSH, with the dashed line indicating the k -th cutoff. These metrics are well defined in Appendix A.2.

3.2 Sparse Attention

For clarity, we restrict our exposition to the case of batch size one with a single query vector $\mathbf{q} \in \mathbb{R}^d$. Consider keys $\mathbf{k}_1, \dots, \mathbf{k}_N \in \mathbb{R}^d$ and corresponding values $\mathbf{v}_1, \dots, \mathbf{v}_N \in \mathbb{R}^d$. We modify (1) to define sparse attention. Let S denote the sequence of k important token indices selected by a method. The sparse attention computation based on this index set is given by:

$$\mathbf{y}_k(\mathbf{q}) = \sum_{i \in S} \alpha_i \mathbf{v}_i. \quad (2)$$

4 Introducing SOCKET

4.1 LSH as a Ranker

In dense attention, a query vector \mathbf{q} interacts with all N keys to produce attention weights, which are then applied to the corresponding N values to generate the output embedding. Prior work has shown that, for token generation, a small subset of keys often dominates the attention mass [53, 16]. We leverage this observation by using soft LSH as a sparsification mechanism, treating it as a scoring function to identify the most relevant keys. In traditional LSH-based retrieval, each key \mathbf{k}_j is projected into L independent hash tables. For each table ℓ , the key is assigned to a discrete bucket $b_j^{(\ell)}$. At inference time, the query \mathbf{q} is hashed in the same manner, and a key is scored by counting the number

Algorithm 1 PrecomputeKeyHashes (prefill)

```

1: Input: Keys  $\{\mathbf{k}_j\}_{j=1}^N \subset \mathbb{R}^d$ , #hyperplanes  $P$ , #tables  $L$ .
2: Set  $R \leftarrow 2^P$ .
3: for  $\ell = 1$  to  $L$  do
4:   Sample  $\mathbf{W}^{(\ell)} \in \mathbb{R}^{P \times d}$  with i.i.d.  $\mathcal{N}(0, 1)$  rows
5:   for  $j = 1$  to  $N$  do
6:      $h^{(\ell)}(\mathbf{k}_j) \leftarrow \text{sign}(\mathbf{W}^{(\ell)} \mathbf{k}_j) \in \{\pm 1\}^P$ 
7:     Encode  $h^{(\ell)}(\mathbf{k}_j)$  as a bucket id  $b_j^{(\ell)} \in [R]$ 
8:   end for
9: end for
10: return  $\{\mathbf{W}^{(\ell)}\}_{\ell=1}^L, \{b_j^{(\ell)}\}_{\ell=1, \dots, L; j=1, \dots, N}$ 

```

Algorithm 2 SoftBucketProbs (decoding)

```

1: Input: Query  $\mathbf{q} \in \mathbb{R}^d$ , tables  $\{\mathbf{W}^{(\ell)}\}_{\ell=1}^L$  with  $\mathbf{W}^{(\ell)} \in \mathbb{R}^{P \times d}$ , corners  $\{\mathbf{c}_r\}_{r=1}^R \subset \{\pm 1\}^P$  where  $R = 2^P$ , temperature  $\tau > 0$ .
2: for  $\ell = 1$  to  $L$  do
3:    $\mathbf{u}^{(\ell)}(\mathbf{q}) \leftarrow \frac{1}{\sqrt{d}} \tanh(\mathbf{W}^{(\ell)} \mathbf{q}) \in \mathbb{R}^P$ 
4:   for  $r = 1$  to  $R$  do
5:      $\text{logit}^{(\ell)}(r) \leftarrow \frac{\mathbf{u}^{(\ell)}(\mathbf{q})^\top \mathbf{c}_r}{\tau}$ 
6:   end for
7:    $p_\tau^{(\ell)}(\cdot | \mathbf{q}) \leftarrow \text{softmax}(\text{logit}^{(\ell)}(1), \dots, \text{logit}^{(\ell)}(R))$ 
8: end for
9: return  $p_\tau^{(\ell)}(r | \mathbf{q})$  for all  $r \in [R]$  and  $\ell \in [L]$ .

```

of hash tables in which it collides with the query:

$$s_{\text{hard}}(\mathbf{k}_j, \mathbf{q}) = \sum_{\ell=1}^L \mathbb{I}[b_j^{(\ell)} = b_{\mathbf{q}}^{(\ell)}], \quad (3)$$

where $\mathbb{I}[\cdot]$ denotes the indicator function. In contrast, our method replaces hard hashing of the query with a soft assignment. While keys are still assigned to a single bucket per hash table, the query distributes probability mass across all buckets. Specifically, for each hash table ℓ , we compute a probability distribution $p(b^{(\ell)} | \mathbf{q})$ over buckets. The resulting soft LSH score for a key \mathbf{k}_j is then defined as

$$s_{\text{soft}}(\mathbf{k}_j, \mathbf{q}) = \sum_{\ell=1}^L p_\tau^{(\ell)}(b_j^{(\ell)} | \mathbf{q}) \quad (4)$$

This formulation assigns higher scores to keys whose hash buckets receive greater probability mass under the query's soft hash. We use these scores to select the top- k keys, on which exact attention is subsequently computed. A clean schematic that distinguishes traditional LSH and soft LSH as a stable ranker can be seen in fig. 1.

4.2 The Final Algorithm

Our method consists of three stages: Keys preprocessing, Query-time scoring, and Sparse attention computation.

Algorithm 3 ValueAwareTop- k Attention $\mathbf{y}_k(\mathbf{q})$

- 1: **Input:** Query \mathbf{q} , BucketProbs $p_\tau^{(\ell)}(r \mid \mathbf{q})$, bucket ids $b_j^{(\ell)}$, values $\mathbf{v}_j \in \mathbb{R}^d$ for all $j \in [N]$, $\ell \in [L]$; # tables L ; budget k .
- 2: **for** $j = 1$ to N **do**
- 3: $\hat{w}_j \leftarrow \sum_{\ell=1}^L p_\tau^{(\ell)}(b_j^{(\ell)} \mid \mathbf{q})$
- 4: **end for**
- 5: $\mathcal{S}_k \leftarrow \text{TopK}(\hat{w}_1 \|\mathbf{v}_1\|_2, \dots, \hat{w}_N \|\mathbf{v}_N\|_2)$
- 6: $\alpha_j \leftarrow \frac{\exp(\hat{w}_j)}{\sum_{i \in \mathcal{S}_k} \exp(\hat{w}_i)}$ for all $j \in \mathcal{S}_k$
- 7: **return** $\mathbf{y}_k(\mathbf{q}) = \sum_{j \in \mathcal{S}_k} \alpha_j \mathbf{v}_j$

Key hashing (prefill): During the prefill phase, each key vector is hashed into L independent hash tables. Specifically, we apply L random projections and assign each key to a single bucket per hash table. These bucket assignments are computed once and stored for reuse during decoding in GPU memory. This procedure is summarized in Algorithm 1.

Query soft hashing and scoring (decoding): At decoding time, a new query vector is softly hashed into the same L hash tables. Instead of a single bucket assignment, the query induces a probability distribution over buckets in each table. Using these distributions, we compute a score for every key by aggregating the probability mass assigned to the key’s corresponding buckets, as defined in (4). This step is illustrated clearly in Algorithm 2.

Top- k selection and attention: Finally, we select the top- k keys according to their soft LSH scores and compute exact attention using only this subset. Algorithm 3 clearly explains this procedure. This yields a sparse yet high-quality approximation of dense attention. We discuss approximation quality in the next section.

5 Theoretical Insights

In this section, we present the theoretical analysis of our method. We characterize the quality of the similarity scores produced by soft LSH and study a sampling-based estimator to establish concentration and approximation guarantees with respect to cosine similarity-based (angular) attention. We adopt angular attention as a modeling choice, as it provides an interpretable and analytically tractable surrogate for the attention scoring function. Concretely, for a fixed query \mathbf{q} and keys $\{\mathbf{k}_j\}_{j=1}^N$, we define the angular kernel weights

$$w_j := \left(1 - \frac{1}{\pi} \cos^{-1} \left(\frac{\mathbf{q}^\top \mathbf{k}_j}{\|\mathbf{q}\| \|\mathbf{k}_j\|} \right)\right)^P \in [0, 1], \quad (5)$$

where P controls the sharpness of the kernel. Normalizing these weights yields the angular attention distribution and the corresponding angular attention output is given by

$$a_j := \frac{w_j}{Z}, \quad Z := \sum_{i=1}^N w_i, \quad \mathbf{y}^* := \sum_{j=1}^N a_j \mathbf{v}_j.$$

Our theoretical analysis aims to approximate this \mathbf{y}^* . Prior work has shown that cosine-similarity kernels amenable to LSH closely match the behavior of softmax attention in practice, and even on

random data [24]. Accordingly, our analysis focuses on this surrogate rather than the full softmax operator. We emphasize that sampling is used purely as an analytical tool: it yields unbiased estimators and enables clean high-probability error bounds. The inference-time procedures described in Algorithms 1 and 2 remain unchanged; for the purpose of analysis, we replace only the final aggregation step with a sampling-based estimator. In practice, during inference with pretrained Transformers (see Section 6), Algorithm 3 deals with deterministic top- k selection using the same soft LSH scores and applies the standard softmax normalization over the selected subset. This preserves the pretrained attention mechanism while differing from the theory only in the subset selection strategy. We note that this sampling method is directly applicable in practice; however, we leave a detailed exploration as future work. In this context, we also emphasize that sampling is introduced only to meet the underlying sparsity budget rather than to enable the approximation itself. Even without sampling, the finite-table soft collision estimator $\mathbf{y}_{\tau,L}(\mathbf{q})$ (defined below) provides a principled approximation to angular attention, with accuracy controlled by L and the soft-bucketization bias. See Remark 4 for a more detailed discussion on this.

5.1 Sampling-based Estimator

Our sampling-based estimator is constructed from the same scores produced in Algorithm 3, namely the soft-LSH weights $\hat{w}_1, \dots, \hat{w}_N$. For the purpose of theoretical analysis, we rescale these scores *by the number of hash tables L* to obtain $\tilde{w}_j := \frac{1}{L} \sum_{\ell=1}^L p_{\tau}^{(\ell)}(b_j^{(\ell)} \mid \mathbf{q}) = \frac{1}{L} \hat{w}_j$ for $j = 1, \dots, N$. To interpret the rescaled scores as an attention distribution, we further normalize $\tilde{a}_j := \frac{\tilde{w}_j}{\tilde{Z}}$ with $\tilde{Z} := \sum_{j=1}^N \tilde{w}_j$ for $j = 1, \dots, N$.

The normalized weights \tilde{a}_j form a probability distribution over keys and serve as our proxy for angular attention coefficients in the theoretical analysis and the resulting attention output

$$\mathbf{y}_{\tau,L}(\mathbf{q}) = \sum_{j=1}^N \tilde{a}_j \mathbf{v}_j. \quad (6)$$

Note that the randomness in $\mathbf{y}_{\tau,L}(\mathbf{q})$ is due to the random hyperplanes for each hash table that we introduced. Consequently, we define the population (single-table) soft-count weight $w_{\tau,j} := \mathbb{E}(s_j^{(1)}(\mathbf{q}))$, the denominator $Z_{\tau} := \sum_{j=1}^N w_{\tau,j}$, and the output $\mathbf{y}_{\tau}(\mathbf{q}) := \sum_{j=1}^N a_{\tau,j} \mathbf{v}_j$, where $a_{\tau,j} = w_{\tau,j}/Z_{\tau}$. Now, we define a sampling distribution $p_j \propto \tilde{a}_j \|\mathbf{v}_j\|_2$, and consider an estimator formed by drawing M independent samples $J_1, \dots, J_M \sim p := (p_1, \dots, p_N)$ and aggregating

$$\mathbf{T}(\mathbf{q}) := \frac{1}{M} \sum_{m=1}^M \frac{\tilde{a}_{J_m}}{p_{J_m}} \mathbf{v}_{J_m}. \quad (7)$$

In the following sections, we analyze $\mathbf{T}(\mathbf{q})$ using standard concentration arguments. Specifically, we bound its deviation from angular attention and show that the implemented top- k procedure can be interpreted as a deterministic approximation that preserves the dominant mass of the induced score distribution.

5.2 Theoretical Analysis

Our analysis relies on the following two standard assumptions on the normalization constants of the attention distribution and the occupancy of hash buckets.

Assumption 1. $Z \geq Z_{\min} > 0$ and $Z_{\tau} \geq Z_{\tau,\min} > 0$.

Assumption 2. For each table $\ell \in [L]$ and bucket $r \in [R]$, the number of elements are bounded i.e.,

$$\# \left\{ j \in [N] : b_j^{(\ell)} = r \right\} \leq B.$$

Assumption 1 is a non-degeneracy condition ensuring that the normalization constants of both angular attention and its soft-count approximation remain bounded away from zero, thereby excluding pathological cases in which the query is nearly orthogonal to all keys and the attention distribution becomes ill-defined. Assumption 2 controls the maximum bucket occupancy per hash table and is standard in analyses of LSH-based methods. Together, these assumptions ensure stable normalization and prevent any single bucket from dominating the score aggregation, enabling meaningful concentration guarantees.

Theorem 3. *Let $\mathbf{q} \in \mathbb{R}^d$ be a fixed query, with keys $\mathbf{k}_1, \dots, \mathbf{k}_N \in \mathbb{R}^d$ and values $\mathbf{v}_1, \dots, \mathbf{v}_N \in \mathbb{R}^d$. Under Assumptions (1) and (2), and for parameters L, M , and τ with $L \geq \frac{2B^2 \log(8/\delta)}{Z_{\tau,\min}^2}$, the estimator $\mathbf{T}(\mathbf{q})$ in eq. (7) satisfies*

$$\|\mathbf{T}(\mathbf{q}) - \mathbf{y}^*(\mathbf{q})\|_2 = \tilde{\mathcal{O}}\left(\frac{1}{\sqrt{M}} + \frac{1}{\sqrt{L}} + \varepsilon_\tau(\mathbf{q})\right) \|\mathbf{V}\|_2,$$

with probability at least $1 - \delta$, where $\mathbf{y}^*(\mathbf{q})$ denotes the target (angular) attention output. Here $\tilde{\mathcal{O}}(\cdot)$ hides a $\sqrt{\log(1/\delta)}$ factor and absolute constants depending only on $(B, Z_{\min}, Z_{\tau,\min})$, and is independent of N, d, L , and M . Moreover, $\varepsilon_\tau(\mathbf{q})$ quantifies the bias introduced by soft bucketization; it depends on τ and P (equivalently $R = 2^P$) and satisfies $\varepsilon_\tau(\mathbf{q}) \rightarrow 0$ as $\tau \rightarrow 0$ for fixed P .

Theorem 3 provides an end-to-end error decomposition for the proposed soft-count attention estimator $\mathbf{T}(\mathbf{q})$. The bound separates the total error into three components: (i) sampling variance arising from the value-aware sampling step, (ii) finite-table approximation error due to using a limited number of hash tables, and (iii) a bias induced by soft bucketization, quantified by $\varepsilon_\tau = \mathbb{E}\left[1 - p_\tau^{(\ell)}(b_q \mid \mathbf{q})\right]$. This decomposition makes explicit how the algorithmic parameters jointly control the different sources of error. Due to space constraints, the complete proof of Theorem 3 is deferred to Appendix B. To provide intuition, the analysis is organized around the following triangle inequality:

$$\|\mathbf{T}(\mathbf{q}) - \mathbf{y}^*(\mathbf{q})\|_2 \leq \|\mathbf{T}(\mathbf{q}) - \mathbf{y}_{\tau,L}(\mathbf{q})\|_2 + \|\mathbf{y}_{\tau,L}(\mathbf{q}) - \mathbf{y}_\tau(\mathbf{q})\|_2 + \|\mathbf{y}_\tau(\mathbf{q}) - \mathbf{y}^*(\mathbf{q})\|_2, \quad (8)$$

which isolates the contributions of sampling variance, finite-table effects, and soft-bucketization bias, respectively. Appendix B revolves around bounding each of them separately.

Role of M and L : The terms $M^{-1/2}$ and $L^{-1/2}$ in Theorem 3 capture two independent variance sources. The $M^{-1/2}$ term arises from the value-aware sampling step and reflects the Monte Carlo error incurred when approximating the soft attention output using M sampled values. The $L^{-1/2}$ term corresponds to the finite-table approximation of the soft collision kernel and quantifies the concentration of the L -table estimator around its population limit. Both terms decay at the standard parametric rate and are independent of the sequence length N , highlighting the scalability of the method. They can be controlled separately depending on computational and memory constraints.

Role of the temperature τ : The term $\varepsilon_\tau(\mathbf{q})$ in Theorem 3 captures the approximation bias induced by soft bucketization. Fix a table ℓ and define the hard SRP bucket of the query by

$$b_q^{(\ell)} := h^{(\ell)}(\mathbf{q}) = \text{sign}(\mathbf{W}^{(\ell)} \mathbf{q}) \in \{\pm 1\}^P$$

Recall that Algorithm 2 defines

$$p_\tau^{(\ell)}(r \mid \mathbf{q}) = \frac{\exp(\mathbf{u}^{(\ell)}(\mathbf{q})^\top \mathbf{c}_r / \tau)}{\sum_{r'=1}^R \exp(\mathbf{u}^{(\ell)}(\mathbf{q})^\top \mathbf{c}_{r'} / \tau)},$$

We define the peaking (non-dominant mass) quantity

$$\varepsilon_\tau(\mathbf{q}) := \mathbb{E}_{\mathbf{W}^{(\ell)}} \left[1 - p_\tau^{(\ell)}(b_q^{(\ell)} \mid \mathbf{q}) \right],$$

which measures how much probability mass the soft bucket distribution assigns to buckets other than the hard query bucket. To see how τ controls this bias, write the bucket logits as $x_r := \mathbf{u}^{(\ell)}(\mathbf{q})^\top \mathbf{c}_r$ for $r \in [R]$, so that $p_\tau^{(\ell)}(r \mid \mathbf{q}) = \exp(x_r/\tau) / \sum_{r'} \exp(x_{r'}/\tau)$. Let $r^* := \arg \max_{r \in [R]} x_r$. Since $\tanh(\cdot)$ is strictly increasing coordinatewise, we have $r^* = b_q^{(\ell)}$, and factoring out the maximum logit yields

$$\begin{aligned} p_\tau^{(\ell)}(b_q \mid \mathbf{q}) &= \frac{\exp(x_{b_q}/\tau)}{\sum_{r=1}^R \exp(x_r/\tau)} \\ &= \frac{1}{1 + \sum_{r \neq b_q} \exp((x_r - x_{b_q})/\tau)} \end{aligned}$$

Because $x_r - x_{b_q} < 0$ for all $r \neq b_q$ and $R = 2^P$ is finite for fixed P , we have $\exp((x_r - x_{b_q})/\tau) \rightarrow 0$ as $\tau \rightarrow 0$, hence $p_\tau^{(\ell)}(b_q \mid \mathbf{q}) \rightarrow 1$ and therefore $\varepsilon_\tau(\mathbf{q}) \rightarrow 0$ as $\tau \rightarrow 0$ (for fixed P). In the opposite extreme $\tau \rightarrow \infty$, we have $\exp(x_r/\tau) = 1 + \mathcal{O}(1/\tau)$ and thus $p_\tau^{(\ell)}(r \mid \mathbf{q}) \rightarrow 1/R$ for all r , i.e., the bucket distribution uniformizes and $\varepsilon_\tau(\mathbf{q}) \rightarrow 1 - 1/R$. Consequently, τ interpolates between hard bucketing ($\tau \rightarrow 0$) and uniform bucket weights ($\tau \rightarrow \infty$), trading approximation bias against smoother, more stable similarity scores at finite τ .

Remark 4 (Error bound without sampling). *If the value-aware sampling step is omitted, the estimator reduces to the finite-table soft-count attention output $\mathbf{y}_{\tau,L}(\mathbf{q})$. In this setting, the randomness arises solely from the L random hash tables, and the sampling variance term in Theorem 3 disappears. Consequently, under the same assumptions and with probability at least $1 - \delta$ over the hash-table randomness, we have*

$$\|\mathbf{y}_{\tau,L}(\mathbf{q}) - \mathbf{y}^*(\mathbf{q})\|_2 = \tilde{\mathcal{O}}\left(\frac{1}{\sqrt{L}} + \varepsilon_\tau(\mathbf{q})\right) \|\mathbf{V}\|_2.$$

The $L^{-1/2}$ term captures the concentration of the finite-table soft-count estimator around its population limit $\mathbf{y}_\tau(\mathbf{q})$, while $\varepsilon_\tau(\mathbf{q})$ quantifies the bias introduced by soft bucketization relative to angular attention. Thus, in the absence of sampling, soft collision aggregation provides a statistically controlled proxy for angular attention, with accuracy governed by the number of hash tables and the temperature parameter.

Table 2: Comparison of dense and sparse attention methods on LongBench (Llama-3.1-8B-Instruct).

Method	Sparsity	NQA	QAS	MFQA	HPQA	WIKI	MUS	GOV	QMSUM	MNews	LCC	Trivia	SamSUM	Count	Retrieval	Repo	AVG
Baseline	Dense	31.05	44.67	55.97	55.40	55.13	29.41	34.77	25.14	26.90	59.8	91.16	43.24	10.0	99.0	53.92	50.3
PQcache	5×	32.78	45.04	54.69	54.05	48.63	24.35	35.28	25.03	27.02	58.12	86.15	22.11	7.85	100	41.22	46.7
	5×	33.49	45.36	50.10	54.20	45.16	26.56	34.16	24.13	27.04	62.85	77.51	32.36	8.63	100	51.74	47.4
	5×	31	46.04	54.30	54.97	50.74	29.7	35.77	24.90	27.57	60.94	87.74	33.76	9.03	100	49.7	49
Quest (pg=16)	10×	30.88	44.27	53.64	52.61	48.01	26.14	34.92	24.57	27.17	59.81	81.89	14.87	8.67	100	44.75	45.9
	10×	32.21	46.20	52.31	54.79	45.98	25.36	34.95	24.28	27.58	57.96	69.28	31.43	6.02	99.43	53.8	46.8
	10×	31.58	46.7	54.54	54.72	48.48	27.79	35.41	25.04	27.39	60.8	86.96	35.7	7.98	100	48.8	48.8

5.3 Why Soft Collisions Yield More Stable Rankings than Hard LSH?

Our inference procedure relies on top- k selection based on aggregated collision scores. Consequently, the relevant performance criterion is not unbiased estimation of a fixed kernel value, but the stability of *relative ordering* among keys at finite L . When two keys have comparable weights, even modest per-table noise can lead to misranking, making ranking stability a more appropriate objective than pointwise accuracy.

Table 3: Comparison of dense and sparse attention methods on LongBench (Qwen3-8B).

Method	Sparsity	NQA	QAS	MFQA	HPQA	WIKI	MUS	GOV	QMSUM	MNews	LCC	Trivia	SamSUM	Count	Retrieval	Repo	AVG
Baseline	Dense	13.16	26.13	33.98	33.23	22.43	19.13	32.11	22.87	24.79	13.98	89.16	42.69	7	100	8.76	36.4
PQcache	5×	13.61	25.87	34.15	33.48	20.68	17.97	31.83	22.53	25.34	15.2	88.29	42.97	7	100	8.76	36.3
Quest	5×	14.25	28	35.77	33.18	23.04	17.39	33.3	23.4	26.18	12.04	82.65	41.48	7	98.67	11.54	36.1
SOCKET	5×	15.39	26.31	34.62	34.88	22.43	19.06	31.98	22.6	25.21	16.55	88.82	43.99	9	100	11.55	37
PQcache	10×	13.99	25.13	33.89	32.42	20.5	16.69	32.3	22.66	24.9	14.82	86.96	43.29	8	100	10.09	36.1
Quest (pg=8)	10×	13.51	24.95	36.49	32.96	22.1	16.38	32.97	22.18	25.69	11.61	73.35	39.38	6	98.17	10.92	34.1
SOCKET	10×	14.95	26.48	34.83	35.12	21.42	18.96	32.86	22.52	25.78	15.25	88.49	43.83	12	100	12.06	36.9

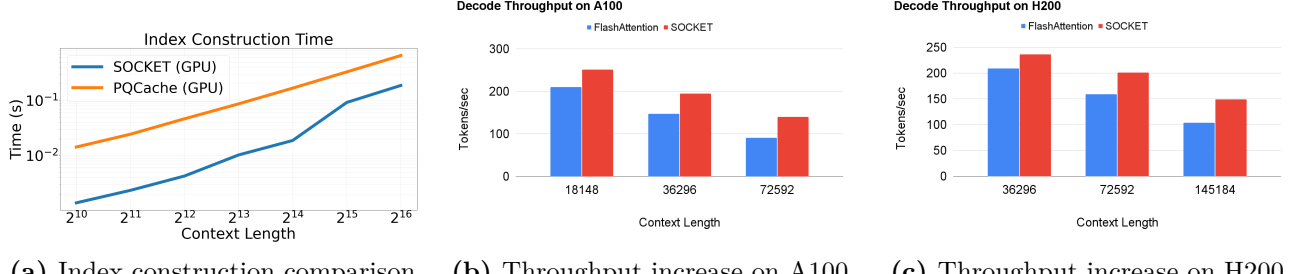


Figure 3: (a) GPU index construction time comparison between SOCKET and PQCache. (b–c) Decode-only throughput versus context length for SOCKET (33× sparsity) and FlashAttention, evaluated using GPT-FAST on Llama-2-7b-hf with a single layer and batch size of 1.

Theorem 3 reveals a central tradeoff: soft bucketization introduces a controllable bias term $\varepsilon_\tau(\mathbf{q})$, while the remaining error terms decay as $L^{-1/2}$ and $M^{-1/2}$. In the hard-bucketing limit $\tau \rightarrow 0$, this bias vanishes and SOCKET reduces to traditional LSH. However, this limit also replaces smooth, graded scores with discrete collision indicators, which discard magnitude information and are maximally noisy at the per-table level. As a result, empirical scores concentrate slowly and induce unstable rankings at finite L , making reliable top- k selection difficult. We formalize this intuition below.

Hard collisions are maximally noisy; soft scores preserve directional structure. Fix a query \mathbf{q} and a key \mathbf{k}_j . For a random table $\mathbf{W}^{(\ell)}$, define the hard collision indicator

$$I_j^{(\ell)} := \mathbf{1}\{b_j^{(\ell)} = b_q^{(\ell)}\} \in \{0, 1\},$$

where $b_q^{(\ell)} = \text{sign}(\mathbf{W}^{(\ell)}\mathbf{q})$. In contrast, SOCKET uses the soft collision score $p_\tau^{(\ell)}(b_j^{(\ell)} \mid \mathbf{q}) \in [0, 1]$. Both quantities are random variables over the randomness of $\mathbf{W}^{(\ell)}$.

Lemma 5. Let X be any random variable supported on $[0, 1]$ with mean $\mathbb{E}[X] = \mu \in [0, 1]$. Then

$$\text{Var}(X) \leq \mu(1 - \mu),$$

with equality if and only if $X \in \{0, 1\}$ with $\mathbb{P}(X = 1) = \mu$.

Lemma 5 shows that Bernoulli indicators are extremal among all $[0, 1]$ -valued surrogates with a given mean, achieving the largest possible variance. Thus, hard LSH employs a maximally noisy per-table surrogate before aggregation.

Lemma 6. Fix a query $\mathbf{q} \in \mathbb{R}^d$ with $\|\mathbf{q}\|_2 = 1$. Let $\{\hat{\mathbf{w}}_i\}_{i=1}^P \subset \mathbb{R}^d$ be unit vectors with $\hat{\mathbf{w}}_i^\top \hat{\mathbf{w}}_j = 0$ for all $i \neq j$, and set $\mathbf{W} := [\hat{\mathbf{w}}_1, \dots, \hat{\mathbf{w}}_P]^\top \in \mathbb{R}^{P \times d}$. Let $\mathbf{k} \sim \mathcal{N}(0, I_d)$ be an independent Gaussian key. For any deterministic scores $s_i = s_i(\mathbf{q}, \hat{\mathbf{w}}_i) \in \mathbb{R}$, define $X := \mathbf{q}^\top \mathbf{k}$ and $Y := \sum_{i=1}^P \text{sign}(\hat{\mathbf{w}}_i^\top \mathbf{k}) s_i$. Then $\mathbb{E}[X] = \mathbb{E}[Y] = 0$, $\mathbb{E}[X^2] = 1$, $\mathbb{E}[Y^2] = \sum_{i=1}^P s_i^2$, and $\mathbb{E}[XY] = C \sum_{i=1}^P (\mathbf{q}^\top \hat{\mathbf{w}}_i) s_i$ with $C = \mathbb{E}|r| = \sqrt{2/\pi}$, $r \sim \mathcal{N}(0, 1)$. Consequently, the correlation between the true similarity signal X and per-table-aggregated hash score Y is given by $\Gamma := C \mathbf{q}^\top \mathbf{W}^\top \hat{\mathbf{s}}$, where $\mathbf{s} := (s_1, \dots, s_P)^\top$, $\hat{\mathbf{s}} := \mathbf{s} / \|\mathbf{s}\|_2$.

Remark 7 (Implication for ranking and top- k selection). *Hard collision indicators and soft scores estimate different quantities, so comparing them as unbiased estimators is not meaningful. However, this distinction is irrelevant for ranking-based inference, as top- k selection depends only on the stability of relative ordering. In this context, Lemma 6 shows that, under approximately orthogonal random projections, the correlation between the true similarity signal X and the single-table aggregated score Y takes the form $\Gamma = C\mathbf{q}^\top \mathbf{W}^\top \hat{\mathbf{s}}$, so ranking behavior is governed by the alignment between the projected query $\mathbf{W}\mathbf{q}$ and the score vector \mathbf{s} . For hard scoring, $\mathbf{s}^{\text{hard}} = \text{sign}(\mathbf{W}\mathbf{q})$, yielding $\Gamma_{\text{hard}} = (C/\sqrt{P})\|\mathbf{W}\mathbf{q}\|_1$, which depends only on the magnitude of the projected coordinates and discards directional information within each orthant. For soft scoring, $\mathbf{s}^{\text{soft}} = \tanh(\mathbf{W}\mathbf{q})$, and in the small-signal regime typical of high-dimensional random projections, $\tanh(\mathbf{W}\mathbf{q}) \approx \mathbf{W}\mathbf{q}$, giving $\Gamma_{\text{soft}} \approx C\|\mathbf{W}\mathbf{q}\|_2$. Since $\|\mathbf{x}\|_1 \leq \sqrt{P}\|\mathbf{x}\|_2$, we have $\Gamma_{\text{hard}} \leq \Gamma_{\text{soft}}$ in this regime, with strict inequality unless the projected coordinates have equal magnitude. Consequently, soft scoring achieves stronger alignment with the true similarity signal, leading to faster concentration of aggregated scores and more stable top- k rankings at finite L , while recovering hard LSH in the zero-temperature limit $\tau \rightarrow 0$ (for fixed P). See Section C for the complete proof of Lemma 6.*

6 Experiments

To ensure broad coverage across models supported by all baselines, we evaluate SOCKET on three widely used long-context, instruction-tuned models of varying scales: Llama-3.1-8B-Instruct [18], Llama-3.2-1B-Instruct [32], and Qwen3-8B [50]. All models support context lengths of up to 128K tokens. We evaluate performance on two complementary benchmarks for long-context understanding: (i) **LongBench** [1], which spans question answering, reasoning, summarization, and code understanding tasks with inputs up to tens of thousands of tokens; and (ii) **RULER** [22], a synthetic diagnostic benchmark designed to assess retrieval of sparse, position-sensitive information embedded in very long contexts. We obtain baseline results from the Skylight benchmark platform.¹ For our experiments, we use the open-source Skylight repository² and implement our method within this framework. Following the evaluation protocol of vAttention [12], we apply dense attention during context processing and sparse attention during question processing and decoding, where the impact of sparsification is most pronounced. Consistent with common practice in the sparse attention literature, we include a small number of sink and local window tokens (e.g., 128 tokens) when computing accuracy in our experiments. The *AVG* score in Tables 2, 3, and 4 excludes Passage-Count and is reported on a 0–100 scale. **Baselines:** We compare SOCKET against five representative sparse attention methods: Quest [42], PQCache [52], HashAttention [13], MagicPig [7], and Double Sparsity [51]. These methods cover a broad spectrum of recent top- k -based and sampling-based sparsification approaches. For all baselines, we use the hyperparameter settings recommended by the respective authors to ensure a fair comparison.

6.1 Effectiveness of SOCKET Across Models

On **Llama-3.1-8B-Instruct**, SOCKET consistently outperforms both Quest and PQCache on LongBench across different sparsity regimes. At 5 \times sparsity, SOCKET achieves an average LongBench score of 49.7, and at 10 \times sparsity it attains 48.8, exceeding the strongest baseline by approximately 2.5 points in both settings. Table 2 shows the average performance of all methods on LongBench without including Passage-Count. Furthermore, SOCKET performs comparably to Quest and PQCache on RULER-32K, and attains the best average at 50 \times sparsity (see Table 1). These gains demonstrate the effectiveness of SOCKET’s soft LSH-based scoring mechanism for selecting important tokens under

¹<https://sky-light.eecs.berkeley.edu/#/home>

²<https://github.com/skylight-org/sparse-attention-hub>

aggressive sparsification.

On the smaller **Llama-3.2-1B-Instruct** model, SOCKET performs competitively with existing baselines. While it does not consistently emerge as the top-performing method with this model, its performance remains on par with data-dependent approaches. This result suggests that, even at smaller model scales where absolute performance differences are narrower, SOCKET’s data-agnostic scoring mechanism remains robust and effective (see Table 4 in Appendix).

Finally, on the **Qwen3-3B** model, SOCKET consistently outperforms both PQCache and Quest across sparsity levels. At $5\times$ sparsity, SOCKET achieves an average score of 37.0, and at $10\times$ sparsity, it attains a comparable score of 36.9. In both regimes, SOCKET exceeds PQCache by approximately 0.6 points and Quest by roughly 2 points (see Table 3). These results further demonstrate that SOCKET serves as a stable ranking mechanism for sparse attention and is suitable for deployment in practical settings as a reliable approximation to dense attention.

6.2 Efficiency of SOCKET

We evaluate the efficiency of SOCKET using decoding throughput on NVIDIA A100 and H200 GPUs. To this end, we modify the GPT-FAST codebase to support sparse attention and report decode-only throughput. Our implementation combines a custom CUDA kernel for key scoring with a Flash Decode Triton kernel to compute attention over the selected keys. Across both hardware platforms, SOCKET delivers consistent throughput gains over FlashAttention [11] that increase with context length. On the H200, SOCKET achieves up to a $1.12\times$ speedup at a context length of 36K tokens, $1.26\times$ at 72K tokens, and up to $1.5\times$ at 145K tokens at $33\times$ sparsity (see fig. 4c). Similarly, on the A100, SOCKET attains a $1.19\times$ speedup at 18K tokens, $1.3\times$ at 36K tokens, and $1.52\times$ at 72K tokens at $33\times$ sparsity (see fig. 4b). These results demonstrate that SOCKET significantly improves decoding efficiency at long context lengths, highlighting its practical advantage for scalable long-context inference.

7 Conclusion

We introduce SOCKET, a Soft Collision Kernel Estimator that enables stable ranking for sparse attention. SOCKET achieves strong long-context performance on LongBench and RULER across three instruction-tuned models. Our optimized CUDA and Triton implementations deliver up to a $1.5\times$ decoding throughput improvement over FlashAttention in GPT-FAST. The soft, data-agnostic design of SOCKET further makes it promising for fine-tuning and downstream tasks, which we leave for future work.

Acknowledgments

The work was primarily supported by Rice Ken Kennedy Institute (K2I) Generative AI Cluster Funding.

References

- [1] Y. Bai, X. Lv, J. Zhang, H. Lyu, J. Tang, Z. Huang, Z. Du, X. Liu, A. Zeng, L. Hou, Y. Dong, J. Tang, and J. Li. LongBench: A bilingual, multitask benchmark for long context understanding. In *Proceedings of the 62nd Annual Meeting of the Association for Computational Linguistics*, Aug. 2024.
- [2] I. Beltagy, M. E. Peters, and A. Cohan. Longformer: The long-document transformer. *arXiv preprint arXiv:2004.05150*, 2020.

- [3] S. Boucheron, G. Lugosi, and P. Massart. *Concentration Inequalities: A Nonasymptotic Theory of Independence*. Oxford University Press, 2013.
- [4] T. B. Brown, B. Mann, N. Ryder, M. Subbiah, et al. Language models are few-shot learners. *Advances in Neural Information Processing Systems*, 2020.
- [5] M. S. Charikar. Similarity estimation techniques from rounding algorithms. In *Proceedings of the 34th Annual ACM Symposium on Theory of Computing (STOC'02)*, pages 380–388. ACM, 2002.
- [6] B. Chen and A. Shrivastava. Densified winner take all (wta) hashing for sparse datasets. In *Proceedings of the 34th Conference on Uncertainty in Artificial Intelligence (UAI)*, 2018.
- [7] Z. Chen, R. Sadhukhan, Z. Ye, Y. Zhou, J. Zhang, N. Nolte, Y. Tian, M. Douze, L. Bottou, Z. Jia, and B. Chen. MagicPIG: Lsh sampling for efficient llm generation. In *International Conference on Learning Representations*. OpenReview.net, 2025.
- [8] A. Chowdhery, S. Narang, J. Devlin, M. Bosma, G. Mishra, A. Roberts, P. Barham, H. W. Chung, C. Sutton, et al. Palm: Scaling language modeling with pathways. *arXiv preprint arXiv:2204.02311*, 2022.
- [9] B. Coleman and A. Shrivastava. Sub-linear RACE sketches for approximate kernel density estimation on streaming data. In *WWW '20: The Web Conference 2020, Taipei, Taiwan, April 20–24, 2020*, pages 1739–1749. ACM / IW3C2, 2020.
- [10] B. Coleman, R. Baraniuk, and A. Shrivastava. Sub-linear memory sketches for near neighbor search on streaming data. In *International Conference on Machine Learning*, 2020.
- [11] T. Dao. Flashattention-2: Faster attention with better parallelism and work partitioning. In *Proceedings of the 37th Conference on Neural Information Processing Systems*, 2023.
- [12] A. Desai, K. K. Agrawal, S. Yang, A. Cuadron, L. G. Schroeder, M. Zaharia, J. E. Gonzalez, and I. Stoica. vattention: Verified sparse attention. *arXiv preprint arXiv:2510.05688*, 2025.
- [13] A. Desai, S. Yang, A. Cuadron, A. Klimovic, M. Zaharia, J. E. Gonzalez, and I. Stoica. Hashattention: Semantic sparsity for faster inference. In *Proceedings of the 42nd International Conference on Machine Learning*, Proceedings of Machine Learning Research (PMLR), pages 13402–13418, 2025. arXiv preprint arXiv:2412.14468.
- [14] J. Devlin, M.-W. Chang, K. Lee, and K. Toutanova. BERT: Pre-training of deep bidirectional transformers for language understanding. In *Proceedings of the 2019 Conference of the North American Chapter of the Association for Computational Linguistics (NAACL)*, pages 4171–4186, 2019.
- [15] Q. Dong, L. Li, D. Dai, C. Zheng, J. Ma, R. Li, H. Xia, J. Xu, Z. Wu, B. Chang, X. Sun, and Z. Sui. A survey on in-context learning. In *Proceedings of the 2024 Conference on Empirical Methods in Natural Language Processing (EMNLP 2024)*, pages 1107–1128. Association for Computational Linguistics, 2024.
- [16] S. Ge, Y. Zhang, L. Liu, M. Zhang, J. Han, and J. Gao. Model tells you what to discard: Adaptive kv cache compression for llms. In *International Conference on Learning Representations*, 2024.
- [17] A. Gionis, P. Indyk, and R. Motwani. Similarity search in high dimensions via hashing. In *Proceedings of the 25th International Conference on Very Large Data Bases (VLDB)*, pages 518–529, Edinburgh, Scotland, UK, 1999. Morgan Kaufmann.
- [18] A. Grattafiori, A. Dubey, A. Jauhri, A. Pandey, A. Kadian, A. Al-Dahle, A. Letman, A. Mathur, A. Schelten, A. Vaughan, A. Fan, A. Goyal, A. Hartshorn, A. Yang, and ... The llama 3 herd of

models. *arXiv preprint arXiv:2407.21783*, 2024. doi: 10.48550/arXiv.2407.21783.

[19] A. Gupta, G. Dar, S. Goodman, D. Ciprut, and J. Berant. Memory-efficient transformers via top-k attention. In *Proceedings of the Second Workshop on Simple and Efficient Natural Language Processing*, 2021.

[20] J. Hoffmann, S. Borgeaud, A. Mensch, E. Buchatskaya, T. Cai, E. Rutherford, D. de las Casas, L. A. Hendricks, J. Welbl, A. Clark, T. Hennigan, E. Noland, K. Millican, G. van den Driessche, B. Damoc, A. Guy, S. Osindero, K. Simonyan, E. Elsen, O. Vinyals, J. W. Rae, and L. Sifre. Training compute-optimal large language models. In *Advances in Neural Information Processing Systems*, 2022.

[21] C. R. C. Hooper, S. Kim, H. Mohammadzadeh, M. Maheswaran, S. Zhao, J. Paik, M. W. Mahoney, K. Keutzer, and A. Gholami. Squeezed attention: Accelerating long context length llm inference. In *Proceedings of the 63rd Annual Meeting of the Association for Computational Linguistics*, pages 32631–32652, 2025.

[22] C.-P. Hsieh, S. Sun, S. Kriman, S. Acharya, D. Rekesh, F. Jia, Y. Zhang, and B. Ginsburg. RULER: What’s the real context size of your long-context language models? In *First Conference on Language Modeling (COLM)*, 2024.

[23] P. Indyk and R. Motwani. Approximate nearest neighbors: Towards removing the curse of dimensionality. In *Proceedings of the Thirtieth Annual ACM Symposium on Theory of Computing*, STOC, pages 604–613. ACM, 1998.

[24] S. Joshi, A. Chowdhury, A. Kanakamedala, E. Singh, E. Tu, and A. Shrivastava. Replacing softmax similarity with a sharpened angular similarity: Theory and practice of scaling to billion-context attention. *arXiv preprint arXiv:2510.04008*, 2025.

[25] J. Jumper, R. Evans, A. Pritzel, et al. Highly accurate protein structure prediction with AlphaFold. *Nature*, 596:583–589, 2021.

[26] N. Kitaev, L. Kaiser, and A. Levskaya. Reformer: The efficient transformer. In *International Conference on Learning Representations*, 2020.

[27] J. Li, D. Li, C. Xiong, and S. C. H. Hoi. Blip-2: Bootstrapping language-image pre-training with frozen image encoders and large language models. *International Conference on Machine Learning*, 2023.

[28] R. Li et al. Starcoder: may the source be with you! *arXiv preprint arXiv:2305.06161*, 2023.

[29] D. Liu, M. Chen, B. Lu, H. Jiang, Z. Han, Q. Zhang, Q. Chen, C. Zhang, B. Ding, K. Zhang, C. Chen, F. Yang, Y. Yang, and L. Qiu. RetrievalAttention: Accelerating long-context llm inference via vector retrieval. In *International Conference on Learning Representations*, 2025.

[30] H. Liu, M. Zaharia, and P. Abbeel. RingAttention with blockwise transformers for near-infinite context. In *International Conference on Learning Representations*, 2024.

[31] W. Liu, J. Wang, S. Kumar, and S.-F. Chang. Hashing with graphs. In *International Conference on Machine Learning*, 2011.

[32] Meta. Llama 3.2: Model cards and prompt formats, 2024. Accessed: 2026-01-24.

[33] OpenAI. GPT-4 technical report. *arXiv preprint arXiv:2303.08774*, 2023.

[34] I. Pinelis. An approach to inequalities for the distributions of infinite-dimensional martingales. In *Probability in Banach Spaces, 8: Proceedings of the Eighth International Conference*, pages 128–134. Springer, 1992.

[35] O. Press, N. Smith, and M. Lewis. Train short, test long: Attention with linear biases enables input length extrapolation. In *International Conference on Learning Representations*, 2022.

[36] A. Radford, J. W. Kim, C. Hallacy, A. Ramesh, G. Goh, S. Agarwal, G. Sastry, A. Askell, P. Mishkin, and J. Clark. Learning transferable visual models from natural language supervision. *Proceedings of the 38th International Conference on Machine Learning*, 2021.

[37] C. Raffel, N. Shazeer, A. Roberts, K. Lee, S. Narang, M. Matena, Y. Zhou, W. Li, and P. J. Liu. Exploring the limits of transfer learning with a unified text-to-text transformer. *Journal of Machine Learning Research*, 21(140):1–67, 2020.

[38] N. Ratner, Y. Levine, Y. Belinkov, O. Ram, I. Magar, O. Abend, E. Karpas, A. Shashua, K. Leyton-Brown, and Y. Shoham. Parallel context windows for large language models. In *Proceedings of the 61st annual meeting of the association for computational linguistics*, pages 6383–6402, 2023.

[39] L. Ruan and Q. Jin. Survey: Transformer based video-language pre-training. *AI Open*, 3:1–13, 2022.

[40] P. Singhania, S. Singh, S. He, S. Feizi, and A. Bhatele. Loki: Low-rank keys for efficient sparse attention. In *Advances in Neural Information Processing Systems*, 2024.

[41] Z. Sun, Y. Yang, and S. Yoo. Sparse attention with learning-to-hash. In *International Conference on Learning Representations*, 2022.

[42] J. Tang, Y. Zhao, K. Zhu, G. Xiao, B. Kasikci, and S. Han. QUEST: Query-aware sparsity for efficient long-context LLM inference. In *International Conference on Machine Learning*, 2024.

[43] H. Touvron, T. Lavril, G. Izacard, X. Martinet, M.-A. Lachaux, T. Lacroix, B. Rozière, N. Goyal, et al. Llama: Open and efficient foundation language models. *arXiv preprint arXiv:2302.13971*, 2023.

[44] A. Vaswani, N. Shazeer, N. Parmar, J. Uszkoreit, L. Jones, A. N. Gomez, L. Kaiser, and I. Polosukhin. Attention is all you need. In *Advances in Neural Information Processing Systems*, 2017.

[45] J. Wei, X. Wang, D. Schuurmans, M. Bosma, F. Xia, E. Chi, Q. V. Le, D. Zhou, et al. Chain-of-thought prompting elicits reasoning in large language models. *Advances in neural information processing systems*, 35:24824–24837, 2022.

[46] C. Xiao, P. Zhang, X. Han, G. Xiao, Y. Lin, Z. Zhang, Z. Liu, and M. Sun. Inflm: Training-free long-context extrapolation for llms with an efficient context memory. In *Advances in Neural Information Processing Systems*, 2024.

[47] G. Xiao, Y. Tian, B. Chen, S. Han, and M. Lewis. Efficient streaming language models with attention sinks. In *International Conference on Learning Representations*, 2024.

[48] J. Yagnik, D. StreLOW, D. A. Ross, and R. Lin. The power of comparative reasoning. In *International Conference on Computer Vision*, pages 2431–2438. IEEE, 2011.

[49] S. Yan, G.-Q. Jiang, Y. Zhang, X. Ma, R. Zhu, C. Cao, and J. Xu. Adamas: Hadamard sparse attention for efficient long-context inference. *arXiv preprint arXiv:2510.18413*, 2025.

[50] A. Yang, A. Li, B. Yang, B. Zhang, B. Hui, B. Zheng, B. Yu, C. Gao, C. Huang, and et al. Qwen3 technical report. *arXiv preprint arXiv:2505.09388*, 2025.

[51] S. Yang, Y. Sheng, J. E. Gonzalez, I. Stoica, and L. Zheng. Post-training sparse attention with double sparsity. *arXiv preprint arXiv:2408.07092*, 2024.

- [52] H. Zhang, X. Ji, Y. Chen, F. Fu, X. Miao, X. Nie, W. Chen, and B. Cui. PQCache: Product quantization-based kvcache for long context llm inference. In *Proceedings of the ACM SIGMOD International Conference on Management of Data*, 2025.
- [53] Z. Zhang, Y. Sheng, T. Zhou, T. Chen, L. Zheng, R. Cai, Z. Song, Y. Tian, C. Ré, C. W. Barrett, Z. Wang, and B. Chen. H₂O: Heavy-hitter oracle for efficient generative inference of large language models. In *Advances in Neural Information Processing Systems 36 (NeurIPS 2023)*, 2023.
- [54] X. Zhou, Z. Sun, and G. Li. DB-GPT: Large language model meets database. *Data Science and Engineering*, 9(1):102–111, 2024.
- [55] K. Zhu, T. Tang, Q. Xu, Y. Gu, Z. Zeng, R. Kadekodi, L. Zhao, A. Li, A. Krishnamurthy, and B. Kasikci. Tactic: Adaptive sparse attention with clustering and distribution fitting for long-context LLMs. *arXiv preprint arXiv:2502.12216*, 2025.

A Appendix

A.1 Additional Notes on Experiments

Table 4: Comparison of dense and sparse attention methods on LongBench (Llama-3.2-1B-Instruct).

Method	Sparsity	NQA	QAS	MFQA	HPQA	WIKI	MUS	GOV	QMSUM	MNews	LCC	Trivia	SamSUM	Count	Retrieval	Repo	AVG
Baseline	Dense	16.12	26.54	42.41	29.31	31.27	14.83	30.14	21.62	25.78	32.51	70.19	7.38	2	4	28.25	27.1
PQcache	5x	15.67	26.56	39.64	31.53	30.47	10.83	28.46	21.45	25.33	41	72.49	6.93	4	4	31.2	27.5
Quest	5x	15.19	24.86	37.96	27.86	27.79	11.19	28.29	21.52	25.05	39.15	69.54	7.55	3.0	4.0	31.19	26.5
SOCKET	5x	14.52	27.61	38.22	28.8	32.87	8.8	28.01	21.56	24.78	39.39	68.69	10.06	4	5	29.73	27
PQcache	10x	14.12	28.16	39.44	31.57	29.2	8.52	27.18	20.62	24.19	41.59	72.52	8.55	4	4	30.8	27.1
Quest (pg=8)	10x	10.61	23.18	35.13	29.47	23.29	10.88	26.95	20.38	24.32	41.46	62.82	10.5	2.0	4.0	32.33	25.3
SOCKET	10x	14.32	25.93	37.84	27.73	31.48	8.55	26.16	20.96	24.5	41.69	69.46	12.93	3	5	29.43	26.8

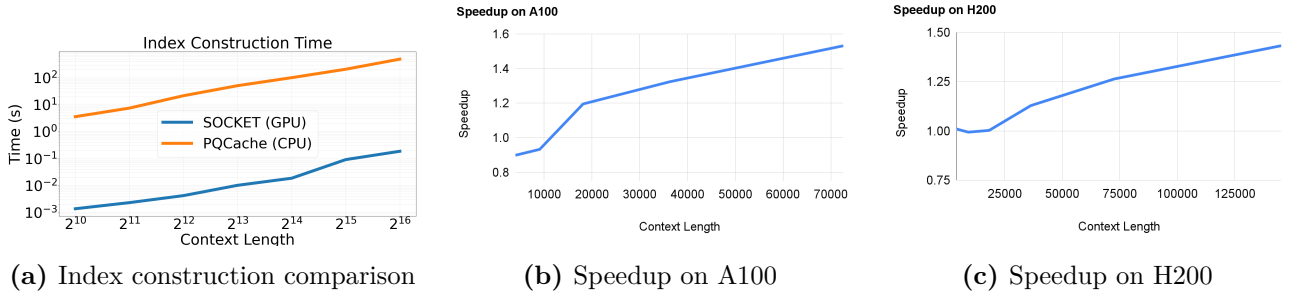


Figure 4: (a) compares the index construction time of SOCKET against a CPU-based PQCache baseline. (b–c) show the throughput speedup of SOCKET over FlashAttention across different hardware platforms.

A.2 Definition of metrics used in fig. 2

Normalized Discounted Cumulative Gain (NDCG): NDCG measures the quality of a ranked list by accounting for both item relevance and ranking position, assigning higher weight to relevant items appearing earlier. Given a ranked list of length k with relevance scores $\{r_i\}_{i=1}^k$, the discounted cumulative gain is defined as

$$\text{DCG} = \sum_{i=1}^k \frac{2^{r_i} - 1}{\log_2(i + 1)}.$$

Let IDCG denote the DCG obtained by sorting items in decreasing order of relevance. The normalized score is then

$$\text{NDCG} = \frac{\text{DCG}}{\text{IDCG}}.$$

Precision: Precision measures the fraction of retrieved items that are relevant. Let S_k denote the set of top- k retrieved items and R the set of relevant items. Precision is defined as

$$\text{Precision} = \frac{|S_k \cap R|}{k}.$$

Jaccard Similarity: Jaccard similarity measures the overlap between two sets. Given two sets A and B , it is defined as

$$\text{Jaccard}(A, B) = \frac{|A \cap B|}{|A \cup B|}.$$

Table 5: Comparison of dense and sparse attention methods on RULER-16K using Llama-3.1-8B-Instruct at 10 \times sparsity. This table is adapted from [12].

	niah_single_1	niah_single_2	niah_single_3	niah_multilkey_1	niah_multiquery	vt	qa_1	qa_2	fwe	niah_multilkey_2	niah_multilkey_3
dense attention	100	100	100	100	97	98.5	97.4	80.5	51.5	93.17	99.5
vAttention (oracle-top- k)	100	100	100	100	97	98	97.5	79.5	51.5	93.17	99.5
oracle-top- k	100	100	100	100	98.5	97.5	97.6	73.5	48	93.17	99.5
vAttention (HashAttention)	100	100	100	100	98	94	96.2	76	48	93.83	98.5
HashAttention	100	100	100	100	99	98	89	73	45.5	91.33	88.5
SOCKET	100	100	100	100	98.25	98.5	88.8	88	54	88.67	98.0
											98.0

Table 6: Hyperparameter settings used across datasets and models.

P	L	τ	Dataset	Model
8	60	0.3-0.7	LongBench	Llama-3.1-8B-Instruct
8	60	0.3-0.7	LongBench	Llama-3.2-1B-Instruct
8	60	0.3-0.7	LongBench	Qwen3-8B
10-12	60	0.3-0.7	RULER-16K	Llama-3.1-8B-Instruct
10-12	60	0.3-0.7	RULER-32K	Llama-3.1-8B-Instruct

B Proof of Theorem 3

B.1 Intermediate Lemmas

Fix a query $\mathbf{q} \in \mathbb{R}^d$, keys $\mathbf{k}_1, \dots, \mathbf{k}_N \in \mathbb{R}^d$ and values $\mathbf{v}_1, \dots, \mathbf{v}_N \in \mathbb{R}^d$. Define the angular kernel weights $w_j = \left(1 - \frac{1}{\pi} \cos^{-1}(\mathbf{q}^\top \mathbf{k}_j / \|\mathbf{q}\| \|\mathbf{k}_j\|)\right)^P \in [0, 1]$ and $Z := \sum_{j=1}^N w_j$. With this, define the angular attention distribution and output:

$$a_j := \frac{w_j}{Z}, \quad \mathbf{y}^*(\mathbf{q}) := \sum_{j=1}^N a_j \mathbf{v}_j.$$

Soft-count distribution: For each table $\ell \in [L]$, draw hyperplanes $\mathbf{W}^{(\ell)} \in \mathbb{R}^{P \times d}$ with i.i.d. $\mathcal{N}(0, 1)$ rows. Let corners $\mathbf{c}_r \in \{\pm 1\}^P$ for $r \in [R]$, $R = 2^P$. Define

$$\mathbf{u}^{(\ell)}(\mathbf{q}) := \frac{1}{\sqrt{d}} \tanh(\mathbf{W}^{(\ell)} \mathbf{q}) \in \mathbb{R}^P, \quad p_\tau^{(\ell)}(r \mid \mathbf{q}) := \frac{\exp(\mathbf{u}^{(\ell)}(\mathbf{q})^\top \mathbf{c}_r / \tau)}{\sum_{r'=1}^R \exp(\mathbf{u}^{(\ell)}(\mathbf{q})^\top \mathbf{c}_{r'} / \tau)}.$$

Let the \mathbf{k}_j 's (hard) bucket id be $b_j^{(\ell)} \in [R]$ (equivalently the sign pattern of $\mathbf{W}^{(\ell)} \mathbf{k}_j$). Define the per-table soft score and the L -table soft-count:

$$s_j^{(\ell)}(\mathbf{q}) := p_\tau^{(\ell)}(b_j^{(\ell)} \mid \mathbf{q}) \in [0, 1], \quad \tilde{w}_j := \frac{1}{L} \sum_{\ell=1}^L s_j^{(\ell)}(\mathbf{q}), \quad \tilde{Z} := \sum_{j=1}^N \tilde{w}_j, \quad \tilde{a}_j := \frac{\tilde{w}_j}{\tilde{Z}}.$$

Now, we define the “soft attention” output: $\mathbf{y}_{\tau,L}(\mathbf{q}) := \sum_{j=1}^N \tilde{a}_j \mathbf{v}_j = \frac{\tilde{n}(\mathbf{q})}{\tilde{Z}} \in \mathbb{R}^d$. Similarly, we define the population (single-table) soft-count weight $w_{\tau,j} := \mathbb{E} [s_j^{(1)}(\mathbf{q})]$, $Z_\tau := \sum_{j=1}^N w_{\tau,j}$, $a_{\tau,j} := \frac{w_{\tau,j}}{Z_\tau}$. Accordingly, the soft-attention output of the population is given by $\mathbf{y}_\tau(\mathbf{q}) := \sum_{j=1}^N a_{\tau,j} \mathbf{v}_j = \frac{\mathbf{n}_\tau(\mathbf{q})}{Z_\tau}$, where the expectations are over the randomness in the table, i.e. $\mathbf{W}^{(\ell)}$ and $\mathbf{n}_\tau(\mathbf{q}) = \sum_{j=1}^N w_{\tau,j} \mathbf{v}_j \in \mathbb{R}^d$.

Note that Assumption 2 directly implies

$$\begin{aligned} Z^{(\ell)}(\mathbf{q}) &:= \sum_{j=1}^N s_j^{(\ell)}(\mathbf{q}) = \sum_{j=1}^N p_\tau^{(\ell)}(b_j^{(\ell)} \mid \mathbf{q}) = \sum_{r=1}^R \sum_{b_j^{(\ell)}=r} p_\tau^{(\ell)}(r \mid \mathbf{q}) \\ &= \sum_{r=1}^R p_\tau^{(\ell)}(r \mid \mathbf{q}) (\sum_{b_j^{(\ell)}=r} 1) \leq B \sum_{r=1}^R p_\tau^{(\ell)}(r \mid \mathbf{q}) = B. \end{aligned} \quad (9)$$

Lemma 8 (Concentration of \tilde{Z} and $\tilde{\mathbf{n}}(\mathbf{q})$). *If $L \geq \frac{2B^2 \log(4/\delta_L)}{Z_{\tau,\min}^2}$, then with probability at least $1 - \delta_L$,*

$$|\tilde{Z} - Z_\tau| \leq B \sqrt{\frac{\log(4/\delta_L)}{2L}} \quad \text{and} \quad \|\tilde{\mathbf{n}} - \mathbf{n}_\tau\|_2 \leq 2\|\mathbf{V}\|_2 \sqrt{2B} \sqrt{\frac{\log(4/\delta_L)}{L}}, \quad (10)$$

and moreover $\tilde{Z} \geq \frac{Z_{\tau,\min}}{2}$.

Proof. Let $\mathbf{V} \in \mathbb{R}^{N \times d}$ be the value matrix such that $\mathbf{V}^\top := [\mathbf{v}_1, \dots, \mathbf{v}_N] \in \mathbb{R}^{d \times N}$. For each table $\ell \in [L]$, define the score vector $\mathbf{s}^{(\ell)}(\mathbf{q}) := (s_1^{(\ell)}(\mathbf{q}), \dots, s_N^{(\ell)}(\mathbf{q}))^\top \in \mathbb{R}^N$ and $\|\mathbf{V}\|_2$ as the spectral norm of \mathbf{V} . From eq. (9), we already know $0 \leq Z^{(\ell)}(\mathbf{q}) \leq B$ for every $\ell \in [L]$. Next, we define the per-table numerator vector $\mathbf{n}^{(\ell)}(\mathbf{q}) := \sum_{j=1}^N s_j^{(\ell)}(\mathbf{q}) \mathbf{v}_j = \mathbf{V}^\top \mathbf{s}^{(\ell)}(\mathbf{q}) \in \mathbb{R}^d$. From the notations we already defined in the beginning of Section B.1, we have

$$\tilde{\mathbf{n}}(\mathbf{q}) = \sum_{j=1}^N \tilde{w}_j \mathbf{v}_j = \frac{1}{L} \sum_{\ell=1}^L \sum_{j=1}^N s_j^{(\ell)}(\mathbf{q}) \mathbf{v}_j = \frac{1}{L} \sum_{\ell=1}^L \mathbf{n}^{(\ell)}(\mathbf{q}) \in \mathbb{R}^d \quad (11)$$

$$\tilde{Z} = \sum_{j=1}^N \tilde{w}_j = \sum_{j=1}^N \left(\frac{1}{L} \sum_{\ell=1}^L s_j^{(\ell)}(\mathbf{q}) \right) = \frac{1}{L} \sum_{\ell=1}^L Z^{(\ell)}(\mathbf{q}). \quad (12)$$

Bounding $\|\mathbf{n}^{(\ell)}(\mathbf{q})\|_2$: Since $0 \leq s_j^{(\ell)}(\mathbf{q}) \leq 1$ for all $j \in [N]$, we have

$$\|\mathbf{s}^{(\ell)}(\mathbf{q})\|_2^2 = \sum_{j=1}^N (s_j^{(\ell)}(\mathbf{q}))^2 \leq \sum_{j=1}^N s_j^{(\ell)}(\mathbf{q}) = Z^{(\ell)}(\mathbf{q}) \leq B. \quad (13)$$

Now, combining eq. (13) and submultiplicativity of the spectral norm, we have

$$\|\mathbf{n}^{(\ell)}(\mathbf{q})\|_2 = \|\mathbf{V}^\top \mathbf{s}^{(\ell)}(\mathbf{q})\|_2 \leq \|\mathbf{V}\|_2 \|\mathbf{s}^{(\ell)}(\mathbf{q})\|_2 \leq \|\mathbf{V}\|_2 \sqrt{B}. \quad (14)$$

Bounding \tilde{Z} : From eq. (9), each $Z^{(\ell)}(\mathbf{q}) \in [0, B]$, and the $Z^{(\ell)}$ are i.i.d. across ℓ with

$$\begin{aligned}\mathbb{E}(\tilde{Z}) &= \mathbb{E}\left(\frac{1}{L} \sum_{\ell=1}^L Z^{(\ell)}(\mathbf{q})\right) = \mathbb{E}(Z^{(\ell)}(\mathbf{q})) \\ &= \mathbb{E}\left(\sum_{j=1}^N s_j^{(\ell)}(\mathbf{q})\right) = \sum_{j=1}^N \mathbb{E}\left(s_j^{(\ell)}(\mathbf{q})\right) \\ &= \sum_{j=1}^N w_{\tau,j} = Z_{\tau}.\end{aligned}\tag{15}$$

Therefore, applying Hoeffding inequality with $t > 0$, we get $\mathbb{P}(|\tilde{Z} - Z_{\tau}| \geq t) \leq 2 \exp\left(-\frac{2Lt^2}{B^2}\right)$. Taking $t = B\sqrt{\frac{\log(4/\delta_L)}{2L}}$, we have

$$\mathbb{P}\left(|\tilde{Z} - Z_{\tau}| \leq B\sqrt{\frac{\log(4/\delta_L)}{2L}}\right) \geq 1 - \delta_L/2.\tag{16}$$

Now, if $B\sqrt{\frac{\log(4/\delta_L)}{2L}} \leq \frac{Z_{\tau,\min}}{2}$ or $L \geq \frac{2B^2 \log(4/\delta_L)}{Z_{\tau,\min}^2}$ then combining Assumption 1 with eq. (16) further boils down to

$$\mathbb{P}\left(\tilde{Z} \geq \frac{Z_{\tau,\min}}{2}\right) \geq 1 - \delta_L/2.\tag{17}$$

Bounding $\tilde{\mathbf{n}}(\mathbf{q})$: Let $\mathbf{X}_{\ell} := \mathbf{n}^{(\ell)}(\mathbf{q}) - \mathbf{n}_{\tau}(\mathbf{q}) \in \mathbb{R}^d$. Then $\mathbb{E}[\mathbf{X}_{\ell}] = 0$ and the \mathbf{X}_{ℓ} are i.i.d. Using eq. (14) and Jensen's inequality, we have

$$\|\mathbf{n}_{\tau}(\mathbf{q})\|_2 = \|\mathbb{E}(\mathbf{n}^{(\ell)}(\mathbf{q}))\|_2 \leq \mathbb{E}\|\mathbf{n}^{(\ell)}(\mathbf{q})\|_2 \leq \|\mathbf{V}\|_2 \sqrt{B}.\tag{18}$$

So, applying triangle inequality on the definition of \mathbf{X}_{ℓ} and combining eqs. (14) & (18) yield

$$\|\mathbf{X}_{\ell}\|_2 \leq \|\mathbf{n}^{(\ell)}(\mathbf{q})\|_2 + \|\mathbf{n}_{\tau}(\mathbf{q})\|_2 \leq 2\|\mathbf{V}\|_2 \sqrt{B}.\tag{19}$$

Next, we apply a vector Hoeffding inequality for sums of bounded mean-zero random vectors in \mathbb{R}^d . Specifically, if $\mathbf{X}_1, \dots, \mathbf{X}_K$ are independent with $\mathbb{E}[\mathbf{X}_k] = 0$ and $\|\mathbf{X}_k\|_2 \leq R$, then

$$\mathbb{P}\left(\left\|\sum_{k=1}^K \mathbf{X}_k\right\|_2 \geq t\right) \leq 2 \exp\left(-\frac{t^2}{2R^2}\right),$$

which follows from *e.g.*, Theorem 3 in [34] and related vector concentration results (e.g., [3]). Applying this in our context directly yields

$$\mathbb{P}(\|\tilde{\mathbf{n}} - \mathbf{n}_{\tau}\|_2 \geq t) \leq 2 \exp\left(-\frac{Lt^2}{8\|\mathbf{V}\|_2^2 B}\right).$$

Setting $t = 2\|\mathbf{V}\|_2 \sqrt{2B} \sqrt{\frac{\log(4/\delta_L)}{L}}$ above yields:

$$\mathbb{P}\left(\|\tilde{\mathbf{n}} - \mathbf{n}_{\tau}\|_2 \leq 2\|\mathbf{V}\|_2 \sqrt{2B} \sqrt{\frac{\log(4/\delta_L)}{L}}\right) \geq 1 - \delta_L/2.\tag{20}$$

Finally, taking the union bound over eqs. (16) and (20) gives the stated joint event with probability at least $1 - \delta_L$, and under $L \geq \frac{2B^2 \log(4/\delta_L)}{Z_{\tau,\min}^2}$ we also have $\tilde{Z} \geq \frac{Z_{\tau,\min}}{2}$ by eq. (17). \square

Lemma 9 (Final bound for $\mathbf{y}_{\tau,L}(\mathbf{q})$). *If $L \geq \frac{2B^2 \log(4/\delta_L)}{Z_{\tau,\min}^2}$, then*

$$\mathbb{P}\left(\|\mathbf{y}_{\tau,L}(\mathbf{q}) - \mathbf{y}_\tau(\mathbf{q})\|_2 \leq C\sqrt{\frac{\log(4/\delta_L)}{L}}\|\mathbf{V}\|_2\right) \geq 1 - \delta_L,$$

where $C = \left(\frac{4\sqrt{2B}}{Z_{\tau,\min}} + \frac{\sqrt{2}B^{3/2}}{Z_{\tau,\min}^2}\right)$.

Proof. Using the definitions of $\mathbf{y}_{\tau,L}(\mathbf{q})$ and $\mathbf{y}_\tau(\mathbf{q})$, and adding and subtracting $\mathbf{n}_\tau/\tilde{Z}$, we have

$$\mathbf{y}_{\tau,L}(\mathbf{q}) - \mathbf{y}_\tau(\mathbf{q}) = \frac{\tilde{\mathbf{n}}}{\tilde{Z}} - \frac{\mathbf{n}_\tau}{Z_\tau} = \frac{\tilde{\mathbf{n}} - \mathbf{n}_\tau}{\tilde{Z}} + \mathbf{n}_\tau \left(\frac{1}{\tilde{Z}} - \frac{1}{Z_\tau}\right). \quad (21)$$

Taking norms both sides and applying triangle inequality yield

$$\|\mathbf{y}_{\tau,L}(\mathbf{q}) - \mathbf{y}_\tau(\mathbf{q})\|_2 \leq \frac{\|\tilde{\mathbf{n}} - \mathbf{n}_\tau\|_2}{\tilde{Z}} + \frac{\|\mathbf{n}_\tau\|_2}{\tilde{Z}Z_\tau} |\tilde{Z} - Z_\tau|. \quad (22)$$

Now using Assumption 1 *i.e.*, $Z_\tau \geq Z_{\tau,\min}$, $\tilde{Z} \geq Z_{\tau,\min}/2$ from Lemma 8, and $\|\mathbf{n}_\tau\|_2 \leq \|\mathbf{V}\|_2\sqrt{B}$ in eq. (18):

$$\|\mathbf{y}_{\tau,L}(\mathbf{q}) - \mathbf{y}_\tau(\mathbf{q})\|_2 \leq \frac{2}{Z_{\tau,\min}} \|\tilde{\mathbf{n}} - \mathbf{n}_\tau\|_2 + \frac{2\|\mathbf{V}\|_2\sqrt{B}}{Z_{\tau,\min}^2} |\tilde{Z} - Z_\tau|. \quad (23)$$

Finally, applying the bounds

$$\|\tilde{\mathbf{n}} - \mathbf{n}_\tau\|_2 \leq 2\|\mathbf{V}\|_2\sqrt{2B} \sqrt{\frac{\log(4/\delta_L)}{L}} \quad \text{and} \quad |\tilde{Z} - Z_\tau| \leq B \sqrt{\frac{\log(4/\delta_L)}{2L}}$$

(which hold jointly with probability at least $1 - \delta_L$ by Lemma 8), we get

$$\begin{aligned} \|\mathbf{y}_{\tau,L}(\mathbf{q}) - \mathbf{y}_\tau(\mathbf{q})\|_2 &\leq \frac{2}{Z_{\tau,\min}} \left(2\|\mathbf{V}\|_2\sqrt{2B} \sqrt{\frac{\log(4/\delta_L)}{L}}\right) + \frac{2\|\mathbf{V}\|_2\sqrt{B}}{Z_{\tau,\min}^2} \left(B \sqrt{\frac{\log(4/\delta_L)}{2L}}\right) \\ &= \left(\frac{4\sqrt{2B}}{Z_{\tau,\min}} + \frac{\sqrt{2}B^{3/2}}{Z_{\tau,\min}^2}\right) \sqrt{\frac{\log(4/\delta_L)}{L}} \|\mathbf{V}\|_2. \end{aligned} \quad (24)$$

This concludes the proof. \square

Conditioned on the tables, define $S_1 := \sum_{j=1}^N \tilde{a}_j \|\mathbf{v}_j\|_2$ and sampling probabilities $p_j := \tilde{a}_j \|\mathbf{v}_j\|_2 / S_1$. Draw i.i.d. indices $J_1, \dots, J_M \sim p$ and define

$$\mathbf{T}(\mathbf{q}) := \frac{1}{M} \sum_{m=1}^M \frac{\tilde{a}_{J_m}}{p_{J_m}} \mathbf{v}_{J_m} \in \mathbb{R}^d.$$

Let $\mathcal{W} = \{\mathbf{W}_1, \dots, \mathbf{W}_L\}$ be the set of random Gaussian hyperplanes with $\mathbf{W}_\ell \in \mathbb{R}^{P \times d}$. Now are ready to present the results for sampling.

Lemma 10. *The following properties hold:*

1. $\mathbb{E}[\mathbf{T}(\mathbf{q}) \mid \mathcal{W}] = \mathbf{y}_{\tau,L}(\mathbf{q})$
2. $\mathbb{P}\left(\|\mathbf{T}(\mathbf{q}) - \mathbf{y}_{\tau,L}(\mathbf{q})\|_2 \leq \|\mathbf{V}\|_2 \sqrt{\frac{8\log(2/\delta_M)}{M}}\right) \geq 1 - \delta_M$

Proof. Proof of Part 1. Let J_1, \dots, J_M be the M independent samples of $\{1, \dots, N\}$ drawn using the probability distribution $p := (p_1, \dots, p_N)$. Define $\mathbf{X}_m := \frac{\tilde{a}_{J_m}}{p_{J_m}} \mathbf{v}_{J_m} \in \mathbb{R}^d$. Then

$$\mathbf{T}(\mathbf{q}) = \frac{1}{M} \sum_{m=1}^M \mathbf{X}_m$$

Now, given \mathcal{W} . Then \tilde{a}_j and p_j are fixed numbers, so:

$$\mathbb{E}[\mathbf{X}_m \mid \mathcal{W}] = \sum_{j=1}^N p_j \frac{\tilde{a}_j}{p_j} \mathbf{v}_j = \sum_{j=1}^N \tilde{a}_j \mathbf{v}_j = \mathbf{y}_{\tau,L}(\mathbf{q}).$$

Therefore,

$$\mathbb{E}[\mathbf{T}(\mathbf{q}) \mid \mathcal{W}] = \frac{1}{M} \sum_{m=1}^M \mathbb{E}[\mathbf{X}_m \mid \mathcal{W}] = \mathbf{y}_{\tau,L}(\mathbf{q})$$

Proof of Part 2. We define the centered random vector $\mathbf{Y}_m := \mathbf{X}_m - \mathbb{E}[\mathbf{X}_m \mid \mathcal{W}] = \mathbf{X}_m - \mathbf{y}_{\tau,L}(\mathbf{q})$. Then $\mathbb{E}[\mathbf{Y}_m \mid \mathcal{W}] = 0$ and $\mathbf{T}(\mathbf{q}) - \mathbf{y}_{\tau,L}(\mathbf{q}) = \frac{1}{M} \sum_{m=1}^M \mathbf{Y}_m$. Now, using $p_{J_m} := \frac{\tilde{a}_{J_m} \|\mathbf{v}_{J_m}\|_2}{S_1}$, we have

$$\|\mathbf{X}_m\|_2 = \left\| \frac{\tilde{a}_{J_m}}{p_{J_m}} \mathbf{v}_{J_m} \right\|_2 = \frac{\tilde{a}_{J_m}}{\tilde{a}_{J_m} \|\mathbf{v}_{J_m}\|_2 / S_1} \|\mathbf{v}_{J_m}\|_2 = S_1 \quad (25)$$

and also applying triangle inequality

$$\|\mathbf{y}_{\tau,L}(\mathbf{q})\|_2 = \left\| \sum_{j=1}^N \tilde{a}_j \mathbf{v}_j \right\|_2 \leq \sum_{j=1}^N \tilde{a}_j \|\mathbf{v}_j\|_2 = S_1. \quad (26)$$

Therefore, applying the triangle inequality on \mathbf{Y}_m , we have

$$\|\mathbf{Y}_m\|_2 \leq \|\mathbf{X}_m\|_2 + \|\mathbf{y}_{\tau,L}(\mathbf{q})\|_2 = 2S_1 \quad (27)$$

Now, note that we can always rewrite $\mathbf{v}_j = \mathbf{V}^T \mathbf{e}_j$ where $\mathbf{e}_j \in \mathbb{R}^N$ is the j -th standard basis vector and thus $\|\mathbf{e}_j\|_2 = 1$. Consequently, applying the submultiplicativity property, we trivially have

$$\|\mathbf{v}_j\|_2 = \|\mathbf{V}^T \mathbf{e}_j\|_2 \leq \|\mathbf{e}_j\|_2 \|\mathbf{V}\|_2 = \|\mathbf{V}\|_2 \quad (28)$$

Using the definition of S_1 , eq. (28) and the fact that $\sum_{j=1}^N \tilde{a}_j = 1$, we get

$$S_1 = \sum_{j=1}^N \tilde{a}_j \|\mathbf{v}_j\|_2 \leq \|\mathbf{V}\|_2 \quad (29)$$

Therefore $\|\mathbf{Y}_m\|_2 \leq 2\|\mathbf{V}\|_2$. Now, using the fact that $\mathbf{T}(\mathbf{q}) - \mathbf{y}_{\tau,L}(\mathbf{q}) = \frac{1}{M} \sum_{m=1}^M \mathbf{Y}_m$ and applying the same vector Hoeffding bound we have

$$\mathbb{P}(\|\mathbf{T}(\mathbf{q}) - \mathbf{y}_{\tau,L}(\mathbf{q})\|_2 \geq t \mid \mathcal{W}) = \mathbb{P}\left(\left\| \frac{1}{M} \sum_{m=1}^M \mathbf{Y}_m \right\|_2 \geq t \mid \mathcal{W}\right) \leq 2 \exp\left(-\frac{Mt^2}{8\|\mathbf{V}\|_2^2}\right) \quad (30)$$

Now, for a failure probability $0 < \delta_M < 1$, we take $t = \sqrt{\frac{8 \log(2/\delta_M)}{M}} \|\mathbf{V}\|_2$ and eq. (30) further simplify to

$$\mathbb{P} \left(\|\mathbf{T}(\mathbf{q}) - \mathbf{y}_{\tau,L}(\mathbf{q})\|_2 \leq \sqrt{\frac{8 \log(2/\delta_M)}{M}} \|\mathbf{V}\|_2 \mid \mathcal{W} \right) \geq 1 - \delta_M \quad (31)$$

Finally, since eq. (31) holds for any \mathcal{W} , we take the expectations over both sides with respect to \mathcal{W} and use the law of iterated expectation to get

$$\mathbb{P} \left(\|\mathbf{T}(\mathbf{q}) - \mathbf{y}_{\tau,L}(\mathbf{q})\|_2 \leq \sqrt{\frac{8 \log(2/\delta_M)}{M}} \|\mathbf{V}\|_2 \right) \geq 1 - \delta_M \quad (32)$$

□

Lemma 11. *For any fixed query \mathbf{q} , we have*

$$\|\mathbf{y}_\tau(\mathbf{q}) - \mathbf{y}^*(\mathbf{q})\|_2 \leq 2B \left(\frac{1}{Z_{\tau,\min}} + \frac{\sqrt{B}}{Z_{\min} Z_{\tau,\min}} \right) \varepsilon_\tau(\mathbf{q}) \|\mathbf{V}\|_2.$$

Proof. From the definition of $\mathbf{y}_\tau(\mathbf{q})$ and $\mathbf{y}^*(\mathbf{q})$ we have

$$\|\mathbf{y}_\tau(\mathbf{q}) - \mathbf{y}^*(\mathbf{q})\|_2 = \left\| \sum_{j=1}^N (a_{\tau,j} - a_j) \mathbf{v}_j \right\|_2 = \left\| \mathbf{V}^\top (\mathbf{a}_\tau - \mathbf{a}) \right\|_2 \leq \|\mathbf{V}\|_2 \|\mathbf{a}_\tau - \mathbf{a}\|_2, \quad (33)$$

where \mathbf{a}_τ and \mathbf{a} are the vectors of order N whose j -th entries are $a_{\tau,j}$ and a_j respectively. We applied the submultiplicativity property of vector and matrix norms in the last inequality of eq. (33). So it remains to bound $\|\mathbf{a}_\tau - \mathbf{a}\|_2$. Now, from the definitions of $a_{\tau,j}$ and a_j in the beginning of Section B.1, we rewrite $(\mathbf{a}_\tau - \mathbf{a})$ as

$$\mathbf{a}_\tau - \mathbf{a} = \frac{\mathbf{w}_\tau}{Z_\tau} - \frac{\mathbf{w}}{Z} = \frac{\mathbf{w}_\tau - \mathbf{w}}{Z_\tau} + \frac{Z - Z_\tau}{Z_\tau Z} \mathbf{w}, \quad (34)$$

where \mathbf{w}_τ and \mathbf{w} are the unnormalized attention vectors of dimension N whose j -th entries are $w_{\tau,j}$ and w_j respectively. The last equality follows from adding and subtracting \mathbf{w}/Z_τ from the second equality and then simplifying. Now, taking ℓ_2 -norm on the both sides of eq. (34) and applying triangle inequality, we further have

$$\begin{aligned} \|\mathbf{a}_\tau - \mathbf{a}\|_2 &\leq \frac{\|\mathbf{w}_\tau - \mathbf{w}\|_2}{Z_\tau} + \frac{|Z - Z_\tau|}{Z_\tau Z} \|\mathbf{w}\|_2 \\ &\leq \frac{\|\mathbf{w}_\tau - \mathbf{w}\|_2}{Z_{\tau,\min}} + \frac{|Z - Z_\tau|}{Z_{\tau,\min} Z_{\min}} \|\mathbf{w}\|_2, \end{aligned} \quad (35)$$

where the last inequality in eq. (35) follows directly from Assumption 1.

Now, we rewrite w_j as an SRP collision probability. Fix a single table with $\mathbf{W}^{(\ell)} \sim \mathcal{N}(0, 1)^{P \times d}$. Define the hard hash (bucket id) of any $\mathbf{x} \in \mathbb{R}^d$ by

$$h(\mathbf{x}) := \text{sign}(\mathbf{W}^{(\ell)} \mathbf{x}) \in \{\pm 1\}^P \quad (\text{equivalently an index in } [R]).$$

Then $b_j^{(\ell)}$ is precisely the index of $h(\mathbf{k}_j)$. Let $b_q := h(\mathbf{q})$ denote the query bucket under the same table. Define the hard collision indicator $I_j := \mathbf{1}\{b_j^{(\ell)} = b_q\} \in \{0, 1\}$. By the standard SRP/SimHash collision identity, we rewrite

$$w_j = \left(1 - \frac{1}{\pi} \cos^{-1} \left(\frac{\mathbf{q}^\top \mathbf{k}_j}{\|\mathbf{q}\| \|\mathbf{k}_j\|} \right) \right)^P = \mathbb{E}[I_j],$$

where the expectation is over $\mathbf{W}^{(\ell)}$. We now express $w_{\tau,j}$ as the soft score expectation and define the peaking quantity. Recall $w_{\tau,j} := \mathbb{E}[s_j^{(\ell)}(\mathbf{q})]$ where $s_j^{(\ell)}(\mathbf{q}) = p_{\tau}^{(\ell)}(b_j^{(\ell)} \mid \mathbf{q}) \in [0, 1]$. For the same table, define the (random) dominant query bucket

$$b_{\star} := \arg \max_{r \in [R]} p_{\tau}^{(\ell)}(r \mid \mathbf{q}).$$

Since $p_{\tau}^{(\ell)}(r \mid \mathbf{q}) \propto \exp(\mathbf{u}^{(\ell)}(\mathbf{q})^{\top} \mathbf{c}_r / \tau)$, $\mathbf{u}^{(\ell)}(\mathbf{q}) = \frac{1}{\sqrt{d}} \tanh(\mathbf{W}^{(\ell)} \mathbf{q})$, and $\tanh(\cdot)$ is strictly increasing, we have $\text{sign}(\mathbf{u}^{(\ell)}(\mathbf{q})) = \text{sign}(\mathbf{W}^{(\ell)} \mathbf{q})$ coordinatewise. Hence the dominant query bucket under soft collision and the hard bucket for \mathbf{q} coincides *i.e.*, $b_{\star} = b_q$. Now, we define the non-dominant mass quantity

$$\varepsilon_{\tau}(\mathbf{q}) := \mathbb{E}[1 - p_{\tau}^{(\ell)}(b_q \mid \mathbf{q})] = \mathbb{E}[1 - p_{\tau}^{(\ell)}(b_{\star} \mid \mathbf{q})],$$

where the expectation is over the randomness of the table $\mathbf{W}^{(\ell)}$. In fact, $\varepsilon_{\tau}(\mathbf{q})$ quantifies how much probability mass the soft bucket distribution assigns to buckets other than the hard SRP bucket, and it controls the discrepancy between soft-count weights and hard collision probabilities.

Now, we are ready to bound $\|\mathbf{w}_{\tau} - \mathbf{w}\|_1$ and $|Z - Z_{\tau}|$ using occupancy B . We first prove a *per-table* inequality. For a fixed realization of $\mathbf{W}^{(\ell)}$, we group indices by buckets and use Assumption 2. Write

$$\sum_{j=1}^N |s_j^{(\ell)}(\mathbf{q}) - I_j| = \sum_{b_j^{(\ell)}=b_q} |p_{\tau}^{(\ell)}(b_q \mid \mathbf{q}) - 1| + \sum_{b_j^{(\ell)} \neq b_q} p_{\tau}^{(\ell)}(b_j^{(\ell)} \mid \mathbf{q}). \quad (36)$$

For the first term, there are at most B indices in bucket b_q , hence

$$\sum_{b_j^{(\ell)}=b_q} |p_{\tau}^{(\ell)}(b_q \mid \mathbf{q}) - 1| = \left(\sum_{b_j^{(\ell)}=b_q} 1 \right) (1 - p_{\tau}^{(\ell)}(b_q \mid \mathbf{q})) \leq B (1 - p_{\tau}^{(\ell)}(b_q \mid \mathbf{q})). \quad (37)$$

For the second term, we regroup by buckets:

$$\sum_{b_j^{(\ell)} \neq b_q} p_{\tau}^{(\ell)}(b_j^{(\ell)} \mid \mathbf{q}) = \sum_{r \neq b_q} \sum_{b_j^{(\ell)}=r} p_{\tau}^{(\ell)}(r \mid \mathbf{q}) \leq \sum_{r \neq b_q} B p_{\tau}^{(\ell)}(r \mid \mathbf{q}) = B (1 - p_{\tau}^{(\ell)}(b_q \mid \mathbf{q})). \quad (38)$$

In the above, the first equality in eq. (38) utilizes the fact that each bucket $r \in [R]$, all keys j with $b_j^{(\ell)} = r$ contribute the same probability value $p_{\tau}^{(\ell)}(r \mid \mathbf{q})$ (because the probability depends only on the bucket r , not on j). Then, inside the inner sum, the term $p_{\tau}^{(\ell)}(r \mid \mathbf{q})$ is constant w.r.t. j and the inequality follows directly from Assumption 2.

Combining eqs. (36), (37) and (38) yield the deterministic bound

$$\sum_{j=1}^N |s_j^{(\ell)}(\mathbf{q}) - I_j| \leq 2B (1 - p_{\tau}^{(\ell)}(b_q \mid \mathbf{q})). \quad (39)$$

Now take expectation over $\mathbf{W}^{(\ell)}$ and use $w_{\tau,j} = \mathbb{E}[s_j^{(\ell)}(\mathbf{q})]$ and $w_j = \mathbb{E}[I_j]$:

$$\begin{aligned} \|\mathbf{w}_{\tau} - \mathbf{w}\|_1 &= \sum_{j=1}^N |w_{\tau,j} - w_j| = \sum_{j=1}^N |\mathbb{E}[s_j^{(\ell)}(\mathbf{q}) - I_j]| \leq \sum_{j=1}^N \mathbb{E}|s_j^{(\ell)}(\mathbf{q}) - I_j| \\ &= \mathbb{E} \left[\sum_{j=1}^N |s_j^{(\ell)}(\mathbf{q}) - I_j| \right] \leq 2B \mathbb{E}[1 - p_{\tau}^{(\ell)}(b_q \mid \mathbf{q})] = 2B \varepsilon_{\tau}(\mathbf{q}). \end{aligned} \quad (40)$$

Since $\|\cdot\|_2 \leq \|\cdot\|_1$, we immediately get

$$\|\mathbf{w}_\tau - \mathbf{w}\|_2 \leq \|\mathbf{w}_\tau - \mathbf{w}\|_1 \leq 2B \varepsilon_\tau(\mathbf{q}). \quad (41)$$

Next, note that $Z = \sum_{j=1}^N w_j$ and $Z_\tau = \sum_{j=1}^N w_{\tau,j}$, hence

$$|Z - Z_\tau| = \left| \sum_{j=1}^N (w_j - w_{\tau,j}) \right| \leq \sum_{j=1}^N |w_j - w_{\tau,j}| = \|\mathbf{w}_\tau - \mathbf{w}\|_1 \leq 2B \varepsilon_\tau(\mathbf{q}). \quad (42)$$

Next, to bound $\|\mathbf{w}\|_2$ using occupancy B , we use that $w_j \in [0, 1]$ and the following shows $Z \leq B$. Indeed, for a fixed table,

$$\sum_{j=1}^N I_j = \#\{j \in [N] : b_j^{(\ell)} = b_q\} \leq B \quad \text{by Assumption 2.}$$

Taking expectation over $\mathbf{W}^{(\ell)}$ gives

$$Z = \sum_{j=1}^N w_j = \sum_{j=1}^N \mathbb{E}[I_j] = \mathbb{E}\left[\sum_{j=1}^N I_j\right] \leq B.$$

Moreover, since $0 \leq w_j \leq 1$,

$$\|\mathbf{w}\|_2^2 = \sum_{j=1}^N w_j^2 \leq \sum_{j=1}^N w_j = Z \leq B,$$

hence

$$\|\mathbf{w}\|_2 \leq \sqrt{B}. \quad (43)$$

Next, we substitute eqs. (41), (42), and (43) into eq. (35):

$$\begin{aligned} \|\mathbf{a}_\tau - \mathbf{a}\|_2 &\leq \frac{\|\mathbf{w}_\tau - \mathbf{w}\|_2}{Z_{\tau,\min}} + \frac{|Z - Z_\tau|}{Z_{\tau,\min} Z_{\min}} \|\mathbf{w}\|_2 \\ &\leq \frac{2B \varepsilon_\tau(\mathbf{q})}{Z_{\tau,\min}} + \frac{2B \varepsilon_\tau(\mathbf{q})}{Z_{\tau,\min} Z_{\min}} \cdot \sqrt{B} \\ &= 2B \left(\frac{1}{Z_{\tau,\min}} + \frac{\sqrt{B}}{Z_{\min} Z_{\tau,\min}} \right) \varepsilon_\tau(\mathbf{q}). \end{aligned} \quad (44)$$

Finally, combining eq. (33) with eq. (44):

$$\|\mathbf{y}_\tau(\mathbf{q}) - \mathbf{y}^*(\mathbf{q})\|_2 \leq \|\mathbf{V}\|_2 \cdot 2B \left(\frac{1}{Z_{\tau,\min}} + \frac{\sqrt{B}}{Z_{\min} Z_{\tau,\min}} \right) \varepsilon_\tau(\mathbf{q}). \quad (45)$$

This proves the lemma. \square

B.2 Proof of Theorem 3

Theorem 12 (Final end-to-end bound via union bound). *Fix a query \mathbf{q} . Suppose Assumptions 1–2 hold and let $\delta_L, \delta_M \in (0, 1)$. Assume*

$$L \geq \frac{2B^2 \log(4/\delta_L)}{Z_{\tau,\min}^2}.$$

Then, with probability at least $1 - (\delta_L + \delta_M)$,

$$\begin{aligned} \|\mathbf{T}(\mathbf{q}) - \mathbf{y}^*(\mathbf{q})\|_2 &\leq \underbrace{\|\mathbf{V}\|_2 \sqrt{\frac{8 \log(2/\delta_M)}{M}}}_{\text{sampling error}} + \underbrace{C \|\mathbf{V}\|_2 \sqrt{\frac{\log(4/\delta_L)}{L}}}_{\text{finite-}L \text{ error}} \\ &\quad + \underbrace{2B \left(\frac{1}{Z_{\tau,\min}} + \frac{\sqrt{B}}{Z_{\min} Z_{\tau,\min}} \right) \varepsilon_\tau(\mathbf{q}) \|\mathbf{V}\|_2}_{\text{soft vs. angular bias}} \end{aligned} \quad (46)$$

where

$$C = \left(\frac{4\sqrt{2B}}{Z_{\tau,\min}} + \frac{\sqrt{2}B^{3/2}}{Z_{\tau,\min}^2} \right), \quad \varepsilon_\tau(\mathbf{q}) = \mathbb{E} \left[1 - p_\tau^{(\ell)}(b_q \mid \mathbf{q}) \right].$$

Proof. By the triangle inequality,

$$\|\mathbf{T}(\mathbf{q}) - \mathbf{y}^*(\mathbf{q})\|_2 \leq \|\mathbf{T}(\mathbf{q}) - \mathbf{y}_{\tau,L}(\mathbf{q})\|_2 + \|\mathbf{y}_{\tau,L}(\mathbf{q}) - \mathbf{y}_\tau(\mathbf{q})\|_2 + \|\mathbf{y}_\tau(\mathbf{q}) - \mathbf{y}^*(\mathbf{q})\|_2. \quad (47)$$

Define the events

$$\begin{aligned} \mathcal{E}_M &:= \left\{ \|\mathbf{T}(\mathbf{q}) - \mathbf{y}_{\tau,L}(\mathbf{q})\|_2 \leq \|\mathbf{V}\|_2 \sqrt{\frac{8 \log(2/\delta_M)}{M}} \right\}, \\ \mathcal{E}_L &:= \left\{ \|\mathbf{y}_{\tau,L}(\mathbf{q}) - \mathbf{y}_\tau(\mathbf{q})\|_2 \leq C \|\mathbf{V}\|_2 \sqrt{\frac{\log(4/\delta_L)}{L}} \right\}. \end{aligned}$$

By the Lemma 10, $\mathbb{P}(\mathcal{E}_M) \geq 1 - \delta_M$, and by Lemma 9, $\mathbb{P}(\mathcal{E}_L) \geq 1 - \delta_L$.

Moreover, Lemma 11 gives the deterministic bound

$$\|\mathbf{y}_\tau(\mathbf{q}) - \mathbf{y}^*(\mathbf{q})\|_2 \leq 2B \left(\frac{1}{Z_{\tau,\min}} + \frac{\sqrt{B}}{Z_{\min} Z_{\tau,\min}} \right) \varepsilon_\tau(\mathbf{q}) \|\mathbf{V}\|_2.$$

On the intersection $\mathcal{E}_M \cap \mathcal{E}_L$, substituting these three bounds into (47) yields the claimed inequality. Finally, by the union bound,

$$\mathbb{P}(\mathcal{E}_M \cap \mathcal{E}_L) \geq 1 - \delta_M - \delta_L. \quad (48)$$

We conclude the proof by taking $\delta_M = \delta_L = \frac{\delta}{2}$ in eq. (48). \square

C Additional Proofs

Proof of Lemma 5. Since $0 \leq X \leq 1$, we have $X^2 \leq X$, hence $\mathbb{E}[X^2] \leq \mathbb{E}[X] = \mu$. Therefore,

$$\text{Var}(X) = \mathbb{E}[X^2] - \mu^2 \leq \mu - \mu^2 = \mu(1 - \mu).$$

If equality holds then $\mathbb{E}[X^2] = \mathbb{E}[X]$, which forces $X^2 = X$, so $X \in \{0, 1\}$ and $\mathbb{P}(X = 1) = \mu$. \square

Proof of Lemma 6. We first note that $X = \mathbf{q}^\top \mathbf{k} \sim \mathcal{N}(0, \|\mathbf{q}\|_2^2) = \mathcal{N}(0, 1)$, hence $\mathbb{E}[X] = 0$ and $\mathbb{E}[X^2] = 1$. Also, for each i , $\hat{\mathbf{w}}_i^\top \mathbf{k} \sim \mathcal{N}(0, 1)$ is symmetric about 0, so $\mathbb{E}[\text{sign}(\hat{\mathbf{w}}_i^\top \mathbf{k})] = 0$ and therefore $\mathbb{E}[Y] = \sum_i s_i \mathbb{E}[\text{sign}(\hat{\mathbf{w}}_i^\top \mathbf{k})] = 0$. For $\mathbb{E}[Y^2]$, expand $Y^2 = \sum_{i=1}^P s_i^2 + \sum_{i \neq j} s_i s_j \text{sign}(\hat{\mathbf{w}}_i^\top \mathbf{k}) \text{sign}(\hat{\mathbf{w}}_j^\top \mathbf{k})$, so $\mathbb{E}[Y^2] = \sum_{i=1}^P s_i^2 + \sum_{i \neq j} s_i s_j \mathbb{E}[\text{sign}(\hat{\mathbf{w}}_i^\top \mathbf{k}) \text{sign}(\hat{\mathbf{w}}_j^\top \mathbf{k})]$. For $i \neq j$, the pair $(\hat{\mathbf{w}}_i^\top \mathbf{k}, \hat{\mathbf{w}}_j^\top \mathbf{k})$ is jointly Gaussian with correlation $\rho_{ij} = \hat{\mathbf{w}}_i^\top \hat{\mathbf{w}}_j$. Using the standard identity $\mathbb{E}[\text{sign}(U) \text{sign}(V)] = \frac{2}{\pi} \arcsin(\rho_{ij})$ for jointly Gaussian (U, V) , and the orthogonality assumption $\rho_{ij} = 0$, we get $\mathbb{E}[\text{sign}(\hat{\mathbf{w}}_i^\top \mathbf{k}) \text{sign}(\hat{\mathbf{w}}_j^\top \mathbf{k})] = 0$; thus all cross terms vanish and $\mathbb{E}[Y^2] = \sum_{i=1}^P s_i^2$.

For $\mathbb{E}[XY]$, by linearity, $\mathbb{E}[XY] = \sum_{i=1}^P s_i \mathbb{E}[(\mathbf{q}^\top \mathbf{k}) \text{sign}(\hat{\mathbf{w}}_i^\top \mathbf{k})]$. Fix i and decompose $\mathbf{k} = r\hat{\mathbf{w}}_i + \mathbf{u}$ where $r := \hat{\mathbf{w}}_i^\top \mathbf{k} \sim \mathcal{N}(0, 1)$ and $\mathbf{u} \perp \hat{\mathbf{w}}_i$ is independent of r . Then $\text{sign}(\hat{\mathbf{w}}_i^\top \mathbf{k}) = \text{sign}(r)$ and $\mathbf{q}^\top \mathbf{k} = r(\mathbf{q}^\top \hat{\mathbf{w}}_i) + \mathbf{q}^\top \mathbf{u}$. By independence and symmetry, $\mathbb{E}[\mathbf{q}^\top \mathbf{u} \cdot \text{sign}(r)] = \mathbb{E}[\mathbf{q}^\top \mathbf{u}] \mathbb{E}[\text{sign}(r)] = 0$. Also $r \text{sign}(r) = |r|$, so $\mathbb{E}[(\mathbf{q}^\top \mathbf{k}) \text{sign}(\hat{\mathbf{w}}_i^\top \mathbf{k})] = (\mathbf{q}^\top \hat{\mathbf{w}}_i) \mathbb{E}|r|$. Summing over i yields $\mathbb{E}[XY] = C \sum_{i=1}^P (\mathbf{q}^\top \hat{\mathbf{w}}_i) s_i$ with $C = \mathbb{E}|r| = \sqrt{2/\pi}$.

Finally, since $\mathbb{E}[X] = \mathbb{E}[Y] = 0$, the correlation is $\Gamma = \frac{\mathbb{E}[XY]}{\sqrt{\mathbb{E}[X^2]\mathbb{E}[Y^2]}} = C \frac{\sum_i (\mathbf{q}^\top \hat{\mathbf{w}}_i) s_i}{\sqrt{\sum_i s_i^2}}$. Writing $\sum_i (\mathbf{q}^\top \hat{\mathbf{w}}_i) s_i = \mathbf{q}^\top \mathbf{W}^\top \mathbf{s}$ and $\|\mathbf{s}\|_2 = \sqrt{\sum_i s_i^2}$ gives $\Gamma = C \mathbf{q}^\top \mathbf{W}^\top \hat{\mathbf{s}}$. \square

Hard vs. soft scoring. Lemma 6 shows that, under approximately orthogonal random planes, the correlation between the true similarity $X = \mathbf{q}^\top \mathbf{k}$ and the aggregated score Y takes the form

$$\Gamma = C \mathbf{q}^\top \mathbf{W}^\top \hat{\mathbf{s}} = C \frac{(\mathbf{W}\mathbf{q})^\top \mathbf{s}}{\|\mathbf{s}\|_2}, \quad C = \sqrt{\frac{2}{\pi}},$$

where $\mathbf{s} = (s_1, \dots, s_P)^\top$ collects the per-plane scores and $\hat{\mathbf{s}} = \mathbf{s}/\|\mathbf{s}\|_2$. Thus, the behavior of the scoring rule is governed by the alignment between the projected query $\mathbf{W}\mathbf{q}$ and the score vector \mathbf{s} .

Hard scoring. For hard LSH, $s_i^{\text{hard}} = \text{sign}(\mathbf{q}^\top \hat{\mathbf{w}}_i)$, equivalently $\mathbf{s}^{\text{hard}} = \text{sign}(\mathbf{W}\mathbf{q})$. In this case $\|\mathbf{s}^{\text{hard}}\|_2 = \sqrt{P}$ and

$$\Gamma_{\text{hard}} = C \frac{(\mathbf{W}\mathbf{q})^\top \text{sign}(\mathbf{W}\mathbf{q})}{\sqrt{P}} = \frac{C}{\sqrt{P}} \|\mathbf{W}\mathbf{q}\|_1.$$

Hence, hard scoring depends only on the ℓ_1 magnitude of the projected coordinates and discards all directional information within each orthant. As a result, small perturbations in $\mathbf{W}\mathbf{q}$ can induce discontinuous changes in $\hat{\mathbf{s}}^{\text{hard}}$, leading to slow concentration and unstable rankings at finite L .

Soft scoring. For soft scoring, $s_i^{\text{soft}} = \tanh(\mathbf{q}^\top \hat{\mathbf{w}}_i)$, i.e., $\mathbf{s}^{\text{soft}} = \tanh(\mathbf{W}\mathbf{q})$ (applied elementwise). The corresponding correlation is

$$\Gamma_{\text{soft}} = C \frac{(\mathbf{W}\mathbf{q})^\top \tanh(\mathbf{W}\mathbf{q})}{\|\tanh(\mathbf{W}\mathbf{q})\|_2}.$$

In the small-signal regime typical of high-dimensional random projections, $|(\mathbf{W}\mathbf{q})_i| \ll 1$ and $\tanh(\mathbf{W}\mathbf{q}) \approx \mathbf{W}\mathbf{q}$, yielding

$$\Gamma_{\text{soft}} \approx C \|\mathbf{W}\mathbf{q}\|_2, \quad \hat{\mathbf{s}}^{\text{soft}} \approx \frac{\mathbf{W}\mathbf{q}}{\|\mathbf{W}\mathbf{q}\|_2}.$$

Thus, soft scoring preserves the directional structure of the projected coordinates and varies smoothly with \mathbf{q} .

Comparison. By the inequality $\|\mathbf{x}\|_1 \leq \sqrt{P}\|\mathbf{x}\|_2$, we have

$$\Gamma_{\text{hard}} = \frac{C}{\sqrt{P}} \|\mathbf{W}\mathbf{q}\|_1 \leq C \|\mathbf{W}\mathbf{q}\|_2 \approx \Gamma_{\text{soft}},$$

with strict inequality unless the coordinates of $\mathbf{W}\mathbf{q}$ have equal magnitude. Consequently, soft scoring achieves strictly stronger alignment with the true similarity signal in the regime relevant for ranking-based inference, explaining its faster concentration and improved top- k stability at finite L .

D Pseudocode for a custom CUDA kernel for scoring keys

Algorithm 4 SoftHashCollisionScores (query-side)

```

1: Input: Query  $\mathbf{q}$ ; BucketProbs  $p_\tau^{(\ell)}(r \mid \mathbf{q})$ ; bucket ids  $b_j^{(\ell)}$ ; Value norms  $\|\mathbf{v}_j\|_2 \geq 0$  for all  $j \in [N]$ ;  

   mask  $m_j \in \{0, 1\}$  indicating whether key  $j$  is valid.  

2: Per-key computation (one thread per  $j$ ):  

3: for  $j = 1$  to  $N$  do  

4:   if  $m_j = 0$  then  

5:      $\hat{w}_j(\mathbf{q}) \leftarrow -\infty$   

6:   else  

7:      $\hat{w}_j(\mathbf{q}) \leftarrow \|\mathbf{v}_j\|_2 \cdot \sum_{\ell=1}^L p_\tau^{(\ell)}(b_j^{(\ell)} \mid \mathbf{q})$   

8:   end if  

9: end for  

10: Output: Collision scores  $\{\hat{w}_j(\mathbf{q})\}_{j=1}^N$  for the  $N$  keys.

```
